

Evidence for distinct stages of magma history recorded by the compositions of accessory apatite and zircon

A.J. Miles^{a,*}, C.M. Graham^a, C.J. Hawkesworth^b, M.R. Gillespie^c, R.W. Hinton^a and EIMF^d

^a*School of GeoSciences, King's Buildings, West Mains Road, University of Edinburgh
Edinburgh, EH9 3JW, UK*

^b*Department of Earth Sciences, University of St Andrews, North Street, St Andrews, KY16
9AL, UK*

^c*British Geological Survey, Murchison House, West Mains Road, Edinburgh, EH9 3LA, UK*

^d*Edinburgh Ion Microprobe Facility, School of GeoSciences, King's Buildings, West Mains
Road, University of Edinburgh Edinburgh, EH9 3JW, UK*

*Corresponding author: Tel.: +44 131 650 5916

Email addresses: Andrew.Miles@ed.ac.uk (A.J. Miles), Colin.Graham@ed.ac.uk (C.M. Graham), mrg@bgs.ac.uk (M.R. Gillespie), chris.hawkesworth@st-andrews.ac.uk (C.J. Hawkesworth), Richard.Hinton@ed.ac.uk (R.W. Hinton), ionprobe@ed.ac.uk (EIMF).

Key Words: Accessory minerals, trace elements, hot zone, granite emplacement, magma ascent, incremental assembly

Abstract

Accessory minerals contain a robust and accessible record of magma evolution. However, they may reflect relatively late stage conditions in the history of the host magmas. In the normally zoned Criffell granitic pluton (Scotland), whole-rock (WR) compositions reflect open system assimilation and fractional crystallisation at depths of > 11 km, whereas amphibole barometry and the absence of inherited zircon suggest that the observed mineral assemblages crystallised following emplacement of magmas with little or no crystal cargo at depths of 4 to 6 km. The crystallisation history is documented by large trace element variations amongst apatite crystals from within individual samples: decreasing LREE and Th concentrations in apatite crystals from metaluminous samples reflect broadly synchronous

crystallisation of allanite, whereas lower LREE and Th, and more negative Nd anomalies in apatites from peraluminous samples reflect the effects of monazite crystallisation. WR evolution is likely to have occurred within a deep crustal hot zone where H₂O-rich (~ 6wt %), low viscosity magmas segregated and ascended adiabatically in a super-liquidus state, leading to resorption of most entrained crystals. Stalling, emplacement and crystallisation resulted from intersection with the H₂O-saturated liquidus at ~ 4 km. H₂O contents are as important as temperature in the development of super-liquidus magmas during ascent, blurring distinctions between apparently ‘hot’ and ‘cold’ granites. The trace element contents of most accessory minerals are controlled by competitive crystallisation of other accessory minerals in small melt batches, consistent with the incremental assembly of large granitic plutons.

1. Introduction

The bulk compositions and differentiation of silicic magmas may be governed by a range of factors, including source rock composition, magma mixing, assimilation of country rocks, fractional melting, fractional crystallisation, water activity and the pressure and temperature pathways of magma evolution (e.g. Bowen, 1928; DePaolo, 1981; Stephens et al. 1985; Gardner et al. 1995; Kemp et al. 2007). However, in order to account for the large volumes of silicic rocks and absence of significant mafic cumulates in the upper crust, it has been proposed that these differentiation processes operate mainly at lower crustal depths (Debari and Coleman, 1989; Kay and Kay, 1993; Müntener et al. 2001; Jull and Keleman, 2001; Coleman et al. 2004; Annen et al. 2006a; Appleby et al. 2008; Kemp et al. 2006a; Kemp et al. 2006b; Ulmer, 2007). This has since been supported by numerical simulations of heat transfer (Annen and Sparks, 2002) and high-temperature experiments (Müntener et al. 2001; Prauteau and Scaillet, 2003) that demonstrate that silica-rich magmas can be generated by incomplete crystallisation of hydrous basalts at lower crustal depths. Furthermore, the liquid-lines-of-descent represented by the whole-rock (WR) compositions of some batholiths can only be simulated by phase equilibria models at lower crustal depths where plagioclase crystallisation is delayed because of elevated pressures (Ulmer, 2007). Differentiation and the determination of bulk magma compositions is thought to occur within hot zones composed of nested sill complexes or small magma chambers (Annen and Sparks, 2002; Annen et al. 2006a; Annen et al. 2006b). By contrast, the mineral assemblages in many volcanic rocks (e.g. Bacon 1983; Bacon and Druitt, 1988; Druitt and Bacon, 1989; Harford et al. 2002; Blundy and Cashman, 2005) have been shown to crystallise in the shallow crust. Experimental data have shown that

the observed phase proportions and their compositions in calc-alkaline magmas are best simulated with near-closed system, polybaric crystallisation of initially fully molten magmas and H₂O-saturated conditions without requiring needing significant decreases in magma temperatures (Blatter and Carmichael, 1998; Martel et al. 1999; Couch et al. 2003; Rutherford and Devine, 2003; Costa et al 2004; Blundy and Cashman, 2005). In many cases, crystallisation is therefore mainly a consequence of decompression rather than decrease in temperature and has been successfully demonstrated by mineral thermometry (e.g. Colima andesite, Moore and Carmichael, 1998), plagioclase compositions (e.g. Soufriere Hills andesite, Higgins and Roberge, 2003; Couch et al, 2003; Rutherford and Devine, 2003) and phenocryst-hosted melt inclusion compositions (e.g. Mount St. Helens, Blundy and Cashman, 2005).

It is therefore likely that WR compositions reflect magmatic processes at depth, while the elemental compositions of most observed mineral phases, including accessory minerals, are mainly determined by the re-distribution of elements between crystallising phases after the emplacement of magma batches at shallower depths.

Accessory minerals such as zircon have been shown to provide a robust record of the evolution of the magmas from which they crystallised, yielding valuable insights into the processes associated with silicic magma genesis and crustal evolution (e.g. Kemp et al. 2006b; Eiler, 2007; Kemp et al. 2007; Appleby et al. 2008; Claiborne et al. 2010; Hawkesworth et al. 2010; Bradley, 2011; Roberts, 2012). Apatite has also been shown to document prolonged compositional changes in silicic magmas (Nash, 1984; Shnukov et al. 1989; Sha and Chappell, 1999; Hoskin et al. 2000; Belousova et al. 2001; Belousova et al. 2002; Chu, et al. 2009). However, the relationship between the trace element compositions recorded in accessory minerals at the crystal scale and those of the WR on a pluton-wide scale is uncertain. Here we examine the processes that control trace element compositions at the WR scale and accessory mineral scale in the normally zoned Criffell pluton, in southern Scotland. We show that in this pluton, accessory mineral crystals and WR trace element compositions appear to record largely different stages of magma history. Based on the observed mineral assemblages, geothermobarometry is used to estimate the temperatures and depths of crystallisation and to examine possible ascent paths and varying physical states of magmas in the Criffell pluton.

2. The Criffell Pluton

The ~20 by ~10 km Criffell pluton was emplaced at ~397 Ma (Halliday, et al. 1980) into low-grade wackes and pelites of Llandovery to Wenlock age (433 to 423 Ma), forming part of the Southern Uplands accretionary prism in southern Scotland (Fig. 1). Criffell belongs to the Trans-Suture Suite (TSS; Brown et al. 2008), which encompasses several plutons on either side of the Iapetus Suture Zone. The plutons were emplaced after final closure of the Iapetus Ocean (Soper and Woodcock, 2003), so despite displaying a calc-alkaline character their genesis cannot be linked directly to subduction. Instead, independent tectonic evidence suggests that pluton emplacement took place during a phase of extension or transtension, possibly in response to oblique convergence between Avalonia and Laurentia (Brown et al. 2008). Further north in Scotland, others have proposed slab break-off following lithospheric thickening as an alternative cause of tectonic subsidence and extension (Atherton and Ghani, 2002; Oliver et al. 2008; Neilson et al. 2009).

Criffell is a normally zoned pluton, with five broadly concentric zones recognised on the basis of changing mineralogical and geochemical character (Stephens, et al. 1985). The three outermost zones (zones 1, 2 and 3) are granodiorite, containing primary hornblende (with occasional cores of clinopyroxene), biotite, plagioclase, potassium feldspar, quartz and accessory allanite, sphene, zircon, apatite and opaque minerals (Fig. 2). Accessory minerals occur mainly as inclusions in all major phases, with apatite also found as inclusions in zircon. The zones become progressively more silicic towards the centre of the intrusion (Stephens and Halliday, 1980), and the two innermost zones (zones 4 and 5) are granite containing primary muscovite and monazite but lacking hornblende, sphene and the abundant zircon and magnetite that characterise the granodiorite. $WR\ SiO_2$ ranges from ~58 wt% in Zone 1 to ~72 wt% in Zone 5. Zones 1 and 2 are metaluminous while zones 3, 4 and 5 are mildly peraluminous. The transition from outer to inner zones is also associated with increasing initial $^{87}Sr/^{86}Sr$ (0.7052 to 0.7073), $\delta^{18}O$ (8.5 to 11.9 ‰) and decreasing ϵNd (-0.6 to -3.1) compositions (Halliday, 1984; Halliday et al. 1980; Stephens et al. 1985). Geochemical modelling of these isotope ratios (Stephens et al. 1985) indicates that such trends may reflect the effects of assimilation of local Southern Uplands sediments and the fractional crystallisation of a crystal assemblage similar to that of mafic enclaves found within the granodiorite. However, $^{207}Pb/^{204}Pb$ isotopes have since shown that the local Southern Uplands sediments into which the pluton is emplaced are unlikely to have contributed to the

crustal signature of the Criffell pluton (Fig. 3) (Thirlwall, 1989). Similarities in the $^{207}\text{Pb}/^{204}\text{Pb}$ compositions of Lake District plutons and those situated north of the Iapetus suture, including Criffell, have been used to suggest they share a common source, the composition of which compares closely with the $^{207}\text{Pb}/^{204}\text{Pb}$ composition of the Skiddaw Group sediments found in the English Lake District to the south (Fig. 3) (Thirlwall, 1989). These conclusions are consistent with seismic evidence for underthrusting of Avalonia beneath the Laurentian margin during the Caledonian Orogeny, potentially as far north as the Midland Valley (Hall, 1984; Beamish and Smythe, 1986; Klemperer and Matthews, 1987; Freeman et al. 1988; Klemperer et al. 1991).

The origins of the configuration of mineralogical and geochemical zones in Criffell remain uncertain. In the outer granodiorites, the alignment of plagioclase, amphibole and biotite crystals gives these rocks a prominent foliation. At a mineral scale, this foliation has been shown to accompany protoclastic textures where small quartz crystals have a mortar texture about larger, kinked plagioclase crystals (Stephens, 1999). Furthermore, the kinking of biotite crystals provides further evidence that strain occurred in the solid state and was not magmatic in origin (Stephens, 1999). Corrioux (1987) suggested that the formation of a foliation in the outer zone of the pluton resulted from the later intrusion of the inner zones, providing evidence for at least two stages of emplacement. WR isotopic variations and discontinuous compositional zones (Stephens et al. 1985; Stephens, 1992) provide further evidence for multiple sources and emplacement episodes. Mafic enclaves are a conspicuous feature of zones 1, 2 and 3; they are isotopically distinct from their host rocks, indicating that they are not the product of crystal settling but instead represent different magmas whose relationship to the WR compositions of the granitic rocks remains unclear (Holden et al. 1987; Holden, 1991).

Apatite is the dominant accessory mineral in all five zones of the Criffell pluton. It forms as euhedral, prismatic crystals between 30 μm and >1 mm in length and occurs mainly as inclusions in other minerals, including zircon. Sphene occurs only in zones 1 and 2 as large (up to 2mm) euhedral crystals making up nearly 2 modal % of the WR (Fig. 2). Euhedral morphology and the scarcity of impingement textures and mineral inclusions indicate that it was an early crystallising phase (Stephens et al. 1985). Allanite and monazite were not observed in thin section, but their presence in very small quantities in mineral separates from metaluminous (Zones 1 and 2) and peraluminous (Zone 5) samples respectively. Zircon in

zones 1 to 4 is seen to occur mainly as solitary, euhedral inclusions up to 200 μm long in all major mineral phases and may also occur as a free crystal phase. Only a very small number of heavily cracked zircon crystals were found in Zone 5. Importantly, the Criffell pluton along with other TSS plutons in Southern Scotland and Northern England lacks inherited zircon. This was shown by an extensive investigation of zircon U-Pb ages, including 17 analyses from four of the TSS granites (Pidgeon and Aftalion, 1978). These findings have since been confirmed by U-Pb dating using Secondary Ionisation Mass Spectrometry (SIMS) on > 100 zircon crystals from the Criffell, Fleet and Shap plutons (Miles et al., in review). SEM imaging also shows no evidence of internal resorption (Fig. 2c and 2d), suggesting that most zircons are not xenocrystic. In this respect, the Criffell pluton (along with other TSS plutons) differs from the numerous Caledonian granite plutons that crop out to the north of the Highland Boundary Fault in Scotland, reflecting either substantial differences in source regions or mineral resorption prior to emplacement (or both).

3. Methodology

Samples were collected from each zone of the Criffell pluton. WR major and trace element concentrations were determined using a PANalytical PW2404 wavelength-dispersive sequential X-ray fluorescence spectrometer at the University of Edinburgh.

Apatite compositions were determined primarily by a Cameca SX-100 electron probe supported for comparative purposes by ion microprobe analyses using a Cameca ims 4f at the University of Edinburgh Ion Microprobe Facility (EIMF). Good agreement was observed between the two methods. Zircon-hosted apatite was analysed in zircons mounted in epoxy blocks following standard zircon separation techniques (see Appleby et al. 2008). Back-scattered electron (BSE) and cathodoluminescence (CL) images were taken on polished surfaces using a Philips XL30P Scanning Electron Microscope (SEM) at the University of Edinburgh. Apatite hosted by other phases was analysed directly in polished thin sections. Allanite mineral separates were identified using SEM energy dispersion x-ray spectroscopy (EDS) analysis (Supplementary material 5).

A wavelength dispersive method (WDS) was used for electron probe analysis of apatite using PC0, LTAP, LPET and LIF dispersion crystals. Beam conditions were 20 kV and 60 nA for trace and most major elements, with a 10 nA defocused beam used to minimise loss of alkalis during analysis.

Apatite inclusions were analysed using the Cameca ims4f ion microprobe, with a 5 nA $^{16}\text{O}^-$ primary ion beam with 15 keV net impact energy and a spot size of approximately 15 μm . Only high energy secondary ions (100-140 eV) were measured in order to reduce molecular ion overlap. F/Ca ion yields were determined using Durango and Wilberforce apatite standards. The very small size of some apatite inclusions in zircon resulted in the need to test for beam overlap with zircon. The very low concentration of Zr in apatite relative to zircon means the magnitude of any overlap can be estimated by taking the ratio of an average zircon Zr concentration (~420,000 ppm) and that of the apatite analysed. Grains that showed evidence for overlap were discounted. Data obtained by both analytical methods (ion probe and electron probe) are similar.

Amphiboles in Zone 1 were analysed in polished thin sections using a wavelength dispersive method (WDS) using a Cameca SX-100 electron probe using LTAP, TAP and PET dispersion crystals. Beam conditions were 25 kV and 10 nA for Na, Mg, Al, Si, K, Ca and Fe, and 15 kV and 100 nA for Ti and Mn.

4. Result

4.1 Whole-rock compositions

WR data are from Stephens and Halliday (1980), Stephens et al. (1985) and this study (Fig. 4; Supplementary material 1). The transition from zones 1 to 5 is associated with decreasing MgO, MnO, Sr, La, Ce, Y, Zr, Ni (Fig. 3) together with TiO_2 , Al_2O_3 , Fe_2O_3 , CaO, P_2O_5 , Nb, Y, Cr, V, Ba, Sc and Nd, and increasing SiO_2 , K_2O , Rb, U and Pb (Supplementary material 1).

WR REE profiles (Stephens et al. 1985) are smooth across all zones with little or no Eu anomaly evident in any zone. WR Ce decreases from 104 ppm to 22 ppm while Y decreases from 26 ppm to 3 ppm with increasing SiO_2 across the entire WR suite (Figs. 4 and 5). LREE/HREE ratios increase with increasing SiO_2 in metaluminous zones, and Ce/Yb ratios increase from 62 to 98. However, in peraluminous zones, Ce/Yb ratios decrease from 97 to 53 with increasing SiO_2 . The Ce-Y array in the WR is steeper than in apatite crystals (Fig. 5), implying different controls on their Ce and Y contents. The progressive decrease in the total

abundance of REE with increasing SiO₂ has been attributed to the removal of small amounts of accessory minerals by fractional crystallisation (Stephens et al. 1985).

4.2 Apatite trace element compositions

Average chondrite-normalised apatite REE profiles (Fig. 6; Supplementary material 2 and 3) and Ce vs Y plots (Fig. 7) for apatite show that crystals from different parts of the pluton yield different Ce-Y trends. Apatites from metaluminous zones (1 and 2) display linearly correlated Y and Ce compositions (Ce: 521 - 3979 ppm; Y <662 ppm) and lack significant Eu anomalies (trend 1) (Fig. 6). By contrast, apatites from peraluminous zones (4 and 5) are relatively depleted in LREE (Ce mostly < 2000 ppm), show larger absolute variations in Y and HREE (Y: 383 - 3054 ppm) (trend 2, Fig. 7) and have prominent negative Eu anomalies (Fig. 6). In Zone 3, a small number of apatite crystals fall on trend 1 and have weak Eu anomalies; they are therefore compositionally similar to apatite crystals in zones 1 and 2. The majority of apatites in Zone 3 fall on trend 2 and are therefore similar to those in zones 4 and 5 (Fig. 7).

In order to compare WR and apatite trace element and REE trends, the Ce and Yb contents of the magmas from which apatites crystallised have been calculated using apatite-melt partition coefficients from Fujimaki et al. (1986) (Fig. 8). Yb has been used in place of Y due to the availability of published Yb partition coefficient data. Like Y in apatite, the Yb concentrations of the melts from which apatites crystallised in individual metaluminous samples are limited in absolute terms relative to Ce (Ce: 90 to 20 ppm; Yb: < 7 ppm) and occupy a similar region of compositional space to that of the WR suite (Fig. 8). In peraluminous zones, calculated Ce-Yb concentrations in the melts in equilibrium with the apatites follow similar trends to those of Ce-Y in apatite (Ce <70 ppm; Yb: 9 to 2 ppm) and contrast markedly with the trend followed by the WR suite (Fig. 8). Yb concentrations in apatite were determined by ion microprobe.

Th and U in apatite decrease from Zone 1 (260-20 and 150-30 ppm, respectively) to Zone 5 (< 10 ppm and < 20 ppm, respectively) (Fig. 9; Supplementary material 3). In general, the Th and U contents of zircon-hosted apatites are higher than for apatite hosted by other phases in each zone (Supplementary material 3). However, beam overlap with enclosing zircon may have affected some analyses, and only data from apatite crystals hosted by Th- and U-poor

minerals (all hosts except for zircon) are plotted in figure 9 and used to infer general trends. Th/U ratios decrease in tandem with Ce in metaluminous zones, but there is little evidence of any correlation in peraluminous zones. Only in intermediate zones (Zones 2 and 3) is there evidence that Th/U ratios correlate with Y (Fig. 9).

5. Discussion

Crustal hot zone models propose that magma compositions are initially determined by open system processes occurring in the deep crust and upper mantle, and that crystallisation and textural evolution occur later in shallow crustal reservoirs (Annen and Sparks, 2002; Annen et al. 2006a; Annen et al. 2006b). The trace element compositions of the earliest accessory minerals to crystallise are therefore likely to reflect those of the bulk magma. However, if accessory minerals crystallise largely in shallow reservoirs, the evolution and subsequent distribution of elements between accessory minerals may be determined by processes that are independent of those that determined the bulk magma composition at depth. Here we examine the extent to which accessory mineral and WR compositions document different stages of magma history.

5.1 Bulk magma variations at depth: whole-rock chemistry

Despite evidence for crustal involvement in the generation of the Criffell magmas (Halliday et al. 1980; Harmon and Halliday, 1980; Halliday, 1984; Stephens and Halliday, 1984; Harmon et al. 1984; Stephens, 1988; Stone and Evans, 1997; Highton, 1999), subsequent $^{207}\text{Pb}/^{204}\text{Pb}$ data (Thirlwall, 1989) have shown that the substantial thickness of Southern Uplands sediments (~11 km; Stephens, 1999) into which the pluton is emplaced cannot have contributed significantly to the crustal signature of these magmas (Fig. 3). Instead, their $^{207}\text{Pb}/^{204}\text{Pb}$ compositions are more similar to those of the Skiddaw Group sedimentary rocks which crop out south of the Iapetus Suture on Avalonian crust (Thirlwall, 1989). Seismic imaging indicates that this Avalonian crust can be traced beneath the southern margin of Laurentia and is present at depths of > 11km beneath the Criffell pluton due to tectonic underthrusting that occurred during final closure of the Iapetus Ocean (Hall, 1984; Beamish and Smythe, 1986; Klemperer and Matthews, 1987; Freeman et al. 1988; Klemperer et al. 1991). The open system magmatic processes responsible for generating the range of WR compositions therefore appear to have occurred at depths of 11 km or more. It follows that

petrological models assuming the local Southern Upland sedimentary rocks are a major crustal contaminant in the Criffell magmas (Stephens et al. 1985) should be re-evaluated.

Petrological modelling of the WR evolution requires knowledge of the crystallising mineral assemblage at depth, in addition to constraints on the composition of potential assimilants. Redox conditions in the amphibole-bearing granodiorites have been shown to lie close to the hematite-magnetite buffer (Stephens et al. 1985) and contain the buffering assemblage necessary for using Al-in-hornblende barometers (Johnson and Rutherford, 1989). The crystallisation of most granitic systems is typically eutectic and most of the buffering assemblage required for hornblende barometry is likely to have crystallised largely simultaneously with amphibole. The results of the Johnson and Rutherford Al-in-hornblende barometer when applied to Zone 1 (Supplementary material 4) reveal that the present mineral assemblage formed at 4 – 6 km (0.8 – 1.5 kbars) depth, within the Southern Uplands accretionary prism. Anderson and Smith (1995) suggest that temperature should also be considered when calculating crystallisation depths using Al-in-hornblende barometers. Crystallisation temperatures have been calculated using the amphibole-plagioclase geothermometer of Blundy and Holland (1990) (albite components are estimated at ~ 75% using optical methods are consistent throughout the samples analysed), revealing crystallisation temperatures between 674°C and 692°C. Using temperature as a further variable and applying the barometer of Anderson and Smith (1995) suggest crystallisation pressures of 2 to 2.4 kbar which equates to ~7 – 9 km depth. Both barometers therefore indicate that the granodiorite mineral assemblage is unlikely to represent the mineral assemblage that was present at the time when most WR compositions were determined at depths > 11 km. Despite strong evidence for significant crustal contamination at depth, the absence of inherited zircons in the Criffell magmas (Pidgeon and Aftalion, 1978) indicates that the current assemblage of accessory phases may also have formed during later stage crystallisation at shallow depths. Their modal proportions and compositions cannot therefore be used to model the evolution of WR compositions at depth.

By contrast, magmatic mafic enclaves that show isotopic disequilibrium with their host granodiorites (Holden et al. 1987; Holden, 1991) in the outer zones of the pluton have been suggested to represent cognate material that may ultimately have been entrained by ascending magmas, providing potential insights into the process of magma differentiation at depth. Following the approach of Stephens et al. (1985), Assimilation and Fractional Crystallisation

(AFC), mixing and fractional crystallisation models have been calculated using a mineral assemblage similar to that of the mafic enclaves (40% plagioclase, 35% amphibole, 20% biotite, 2.5% sphene, 2% apatite and 0.5% zircon) and Skiddaw Group sedimentary rocks as a crustal contaminant (Ce = 35 ppm, Y = 86 ppm; Cooper et al. 1988). Granodiorite sample 244 (Stephens et al. 1985) has been used as a starting composition (Ce = 98 ppm, Y = 13 ppm). Despite uncertainties regarding the origin of the mafic enclaves, AFC processes involving an assemblage identical or similar to that of the mafic enclaves coupled with assimilation of Skiddaw Group (or similar) materials with an assimilation to fractional crystallisation ratio of 0.3 provides the best fit to the trend of decreasing Ce and Y exhibited by the WR suite (Fig. 5). Further uncertainties may result from inferences and estimates of some partition coefficients due to an absence of published data.

5.2 Late-stage crystallisation history at shallow levels: apatite mineral compositions

While WR compositions appear to reflect open system differentiation at depth, it is unclear whether or not shallow level crystallisation processes involved further changes to the WR compositions. The trace element compositions of apatite have previously been shown to archive the petrogenetic history of granitic magmas (Nash, 1984; Shnukov et al. 1989; Sha and Chappell, 1999; Hoskin et al. 2000; Belousova et al. 2001; 2002; Chu et al. 2009). If, like zircon and hornblende, apatite formed during crystallisation at shallower levels and saturated from the bulk magma, then apatite compositions provide a way of determining the crystallisation history of the Criffell magmas that may not always be recorded by WR compositions. Ce-Y trends reveal that apatites from single samples would appear to have crystallised from melts with up to two orders of magnitude variability in Ce and Y contents (Fig. 5). Here we examine the processes by which such compositional diversity is attained and the extent to which apatite retains evidence of magma processes that are distinct from – and independent of – those recorded by WR compositions.

5.3 Apatite saturation

Apatite crystals occur almost exclusively as inclusions in different host minerals and it is possible that they crystallised at the crystal-melt interface during phenocryst growth under locally saturated conditions or in late-stage interstitial melt pools (Bacon, 1989; Hoskin et al.

2000). Local saturation of apatite may prevent crystals from documenting compositions that reflect the bulk magma. This is because local concentration gradients may occur adjacent to growing phenocrysts while the highly evolved compositions of late-stage interstitial melts may bear little resemblance to bulk magma composition. Furthermore, interstitial melts may crystallise under lower temperatures, thereby changing the way some trace elements partition into accessory phases (Hoskin et al. 2000). It is therefore important to determine if apatite became saturated in, and crystallised from, the bulk magma or from local pockets of magma that were isolated from the bulk magma or adjacent to growing phenocrysts. Crystal morphology alone is not enough to distinguish crystals formed in these two settings (Bacon, 1989). In isolated interstitial melt pockets, melt compositions are likely to be more variable and a range of accessory minerals would be expected to saturate sequentially. However, in the Criffell pluton the overwhelming majority of apatite inclusions are found in isolation from other accessory minerals, consistent with crystallisation from the bulk magma. Furthermore, the existence of distinctive and continuous trends as opposed to more random distributions of apatite compositions supports the maintenance of chemical connectivity between apatites and the bulk magma rather than growth at phenocryst interfaces. We therefore favour bulk saturation in all zones of the Criffell pluton.

5.4 Causes of compositional diversity in apatites in metaluminous granites

In order to model the range of Ce-Y compositions exhibited by apatites from single metaluminous samples (Fig. 5), it is first necessary to investigate how their concentrations vary in response to crystallisation. WR compositions, which are considered to be representative of magma compositions at the time of emplacement, are similar to those from which only the most Ce-rich apatites crystallised in zones 1 and 2 (Fig. 8). Crystallisation therefore appears to have induced a trend from high to low Ce concentrations in apatites within these zones, consistent with the common occurrence of decreasing REE concentrations with increasing crystallisation found in other granites that result from the fractionation of REE by accessory minerals (Stephens et al. 1985; Sha and Chappell, 1999; Hoskin et al. 2000; Belousova et al. 2001; Chu et al. 2009).

Other studies have shown that REE diversity in apatites may also result from an increase in partition coefficients between apatite and silicate melts with increasing differentiation, SiO₂ and polymerisation (Prowatke and Klemme, 2006). In this model, increased differentiation in the absence of other accessory minerals should lead to an *increase* in the REE content of apatite. However, the observed trend is one of *depletion* in REE with increasing crystallisation (Figs. 7 and 8). Furthermore, the change from metaluminous to peraluminous zones is associated with only small variations in SiO₂ (<3 wt %) despite large changes in the REE patterns of apatite crystals. Any effect of increasing SiO₂ on the partitioning of REE in apatites from single samples is therefore considered to be of secondary importance.

Having concluded that the observed trends in apatite compositions may also reflect the crystallisation of other accessory phases, the range of compositions observed within single samples may be modelled in terms of the re-distribution of REE amongst competing accessory phases during crystallisation.

Assuming a starting composition similar to that of the WR, no reasonable combination of petrographically observed minerals is capable of reproducing the observed trend of Ce depletion seen in the calculated melt compositions from which apatites in single metaluminous samples crystallised. For example, assuming modal proportions of 40% plagioclase, 20% amphibole, 2.5% sphene, 2% apatite and 0.5% zircon (and using the published partition coefficient data of Fujimaki et al. 1984; Fujimaki, 1986; Sisson, 1994; Tiepolo et al. 2002; Sano et al. 2002), only around half the observed decrease in Ce concentration is predicted after 95% crystallisation.

Another accessory mineral found only in magnetic heavy mineral separates (but not petrographically) from zones 1 and 2 that is also commonly stabilised in metaluminous magmas is allanite (Montel, 1986). Allanite is highly effective at removing LREE, with mineral-melt partition coefficients as high as ~ 2800 (Mahood and Hildreth, 1983). By contrast, there is a minimal difference in the efficiency of HREE removal by allanite relative to apatite. Allanite crystallisation is also consistent with the overall decrease in the Th content and Th/U ratios of apatite in these zones (positive correlations between Ce and Th in apatites have R² values of ~ 0.7 to 0.9) (Fig. 9). The latter decrease in Th/U is likely to reflect increased partitioning of Th relative to U in allanite (Hoskin et al. 2000). Crystallisation models indicate that the observed trend in Ce depletion seen in calculated melt compositions

can be replicated after ~ 40% crystallisation by the additional crystallisation of only 0.1% allanite (Fig. 8) and demonstrates the ability of allanite to generate cryptic signatures of its presence in the Ce and Y contents of apatite.

Experimental studies suggest that even for relatively modest concentrations of LREE, allanite is easily saturated in silicate rocks at relatively low temperatures (~700°C) (Klimm et al. 2008). Furthermore, Janots et al. (2007) calculated that allanite is stable at temperatures as low as 250°C in pelites with 0.88 wt % CaO and 700 ppm LREE. At higher CaO contents such as those of the Criffell magmas, allanite should easily be stabilised. Monazite crystallisation may also effectively reduce the concentration of LREE in granitic magmas, but is seldom saturated in metaluminous magmas (Montel, 1986). Furthermore, the preferential uptake of Nd relative to other REE by monazite commonly results in negative Nd anomalies in other crystallising phases (Sha and Chappell, 1999; Chu et al. 2009). No significant negative WR-normalised Nd anomalies are observed in metaluminous apatites (Fig. 6 and 10). We therefore consider allanite the more likely LREE-controlling co-existing phase in metaluminous zones.

5.5 Might the WR and accessory mineral compositions have been determined together in the metaluminous magmas?

The suggestion that allanite was part of the crystallisation assemblage at shallow levels encourages us to look again at whether it was also present during the development of the WR compositions.

AFC models that assume a crystallisation assemblage similar to that of mafic enclaves coupled with assimilation of Skiddaw Group sedimentary rocks are capable of generating the observed range of WR compositions without allanite crystallisation (Fig. 5). Furthermore, the preference exhibited by allanite for LREE relative to HREE means that if allanite crystallisation was a dominant control on WR differentiation, as is apparently the case during the crystallisation of apatite, more evolved metaluminous WRs (with higher SiO₂) would have *lower* LREE/HREE ratios. LREE/HREE ratios in the metaluminous WR suite *increase* with progressive differentiation and have been interpreted by Stephens et al. (1985) to reflect a dominant amphibole control rather than allanite, but may also reflect zircon crystallisation.

It therefore seems likely that independent processes determined both WR and apatite trace element compositions in distinct regions of the magmatic system, consistent with other evidence suggesting that WR Pb isotope compositions (Fig. 3) were determined at significantly greater depths than those at which crystallisation of amphibole and zircon occurred in the granodiorites.

5.6 Causes of compositional diversity in apatites in peraluminous granites

Apatite crystals from peraluminous zones (zones 4 and 5) define a second trend of variable Y (and Yb) and low Ce relative to those in metaluminous zones (trend 2, Fig. 7) but have indistinguishable textural relations with their host phases. This trend is distinct from that defined by the entire WR suite (Figs. 5, 7 and 8) and indicates that independent magmatic processes have determined the evolutionary trends of WR and crystal compositions in these zones. Apatites in other peraluminous plutons have been shown to define similar compositional trends (Sha and Chappell, 1999; Hoskin et al. 2000; Belousova et al. 2001; 2002; Chu et al. 2009) reflecting the crystallisation of LREE-rich monazite. Monazite is known to saturate readily in peraluminous, two-mica granites. This is supported by evidence that WR compositions in Zones 4 and 5 fall within the experimentally constrained field for monazite saturation (Montel, 1986). Furthermore, small amounts of monazite were recovered from mineral separates from Zone 5. Apatites in zones 4 and 5 commonly display more negative WR-normalised Nd anomalies than those from metaluminous zones (Fig. 10), implying that monazite crystallisation may have imposed compositional controls over the REE compositions of apatite and other co-existing phases. The consistent absence of such Nd anomalies in the WR suite, including in the most evolved and peraluminous WR, indicates that such signatures were not inherited from the WR and that monazite has not influenced WR compositions during AFC processes at depth. The consistently low concentrations of Ce and Th in apatite (Fig. 9) and the absence of further depletion of these elements during apatite crystallisation in zones 4 and 5 suggest that most monazite crystallisation preceded that of apatite in these magmas. Crystallisation of monazite and apatite at different stages of crystallisation may seem contrary to most eutectic systems. However, peraluminous WR compositions in these zones favour early saturation of monazite (Montel, 1986) while the low abundance of CaO (often < 1 wt %) in the most peraluminous zones is likely to have delayed

apatite crystallisation. London (1992) suggested that monazite crystallisation may slow or cease completely once P is accommodated in additional apatite and plagioclase during later stages of crystallisation.

In addition to having crystallised from Ce-depleted melts, apatites from peraluminous magmas commonly have higher HREE contents than are consistent with the HREE contents of the WR. This effect is difficult to explain but may to some extent reflect the absence of major phases such as amphibole (in which HREE are also compatible). Crystallisation of apatite and zircon in Zone 4 is likely to have resulted in Y (and Yb) depletion. Crystallisation alone is therefore likely to induce a progression from high to low Y and Yb concentrations in apatite (Fig. 7 and Fig. 8).

In summary, the similarity in the textural relationship between apatite and host phases in all zones of the pluton, the absence of monazite control in determining WR compositions in peraluminous zones, and the absence of inherited zircon are all consistent with a model where WR and accessory mineral compositions are largely determined separately during different stages of magma history.

5.7 Causes of compositional diversity in apatites from a transitional zone (Zone 3)

The compositions of most of the apatites analysed from Zone 3 resemble those of zones 4 and 5, and presumably also reflect the effects of monazite crystallisation. However, the compositions of a small number of apatite grains resemble those in zones 1 and 2 (Figs. 7 and 8). The WR suite indicates that the transition from metaluminous to peraluminous compositions is associated with progressive differentiation. The presence of apatite compositions in Zone 3 on both trends shows that in this zone early crystallisation is likely to have been dominated by allanite, while apatites that crystallised later were subject to the effects of monazite crystallisation. This is consistent with the stabilisation of monazite relative to allanite in more peraluminous magmas (Montel, 1986).

6. Magma generation, ascent and pluton emplacement

The production of chemically diverse WR compositions within deep-seated regions of the crust followed by crystallisation of the observed mineral phases at shallower depths is consistent with the crustal hot zone model (Annen and Sparks, 2002; Annen et al. 2006a; Annen et al. 2006b). In this model, magmas of silicic and intermediate composition are generated through the repeated intrusion of sills formed from mantle melts that differentiate that causes partial melting of pre-existing and hydrous host rocks and sills. A wide range of WR trace element concentrations, isotopic compositions and water contents can then be generated through the mixing of residual hydrous mafic melts and crustal partial melts. The volumes and rates of melt production depend largely on the volumes of intruded mantle-derived material and how readily the crust fuses, which are in turn broadly dependent on the depths of sill emplacement, temperatures, crustal composition and water activity. Hydrous mafic sills act primarily as a heat and water source for subsequent melt generation, and as such may not necessarily be a dominant component in the newly formed silicic magmas.

Pidgeon and Aftalion (1978) found no geochronological evidence of zircon xenocrysts in any of the post-Caledonian plutons emplaced south of the Highland Boundary Fault (a total of 17 analyses). These findings have since been confirmed by recent U-Pb dating of > 100 zircon crystals from three TSS granites, including the Criffell pluton (Miles et al. *in review*). Though not unique, and with the possible exception of the mafic enclaves, the granitic rocks of the Criffell pluton and other plutons south of the Highland Boundary Fault are relatively unusual amongst the Caledonian granite plutons of northern Britain in lacking inherited crystals from the source regions and the hot zone in which differentiation is likely to have taken place. The paradox is further reinforced by evidence that the Criffell magmas satisfy many of the conditions used to identify low temperature silicic magmas that usually contain a significant inherited component, such as the continued decrease in WR Zr with increasing SiO₂ (Fig. 4) used by Chappell et al. (2004) to identify low temperature granites and persistent zircon saturation. The absence of chemical evidence for either monazite or allanite having affected WR compositions despite their likely involvement in controlling REE distributions amongst accessory minerals during final crystallisation also alludes to an absence of inherited crystals. Furthermore, amphibole-plagioclase thermometry (Blundy and Holland, 1990) applied to granodiorites in Zone 1 (Supplementary material 4) indicates temperatures of $\sim 680 \pm 5^{\circ}\text{C}$ (error quoted as 1 SD for the analysed population; thermometer uncertainty is $\pm 75^{\circ}\text{C}$). These results suggest that inherited zircon grains (along with other accessory minerals) should form a considerable proportion of the crystal population in the Criffell pluton given WR isotopic

evidence for supracrustal contamination (Halliday et al. 1980; Harmon and Halliday, 1980; Halliday, 1984; Harmon et al. 1984; Stephens and Halliday, 1984; Stephens, 1988; Thirlwall, 1989; Stone and Evans, 1997; Highton, 1999).

In the absence of inherited zircon, zircon saturation temperatures (Watson and Harrison, 1983) of $\sim 745^{\circ}\text{C}$ ($\pm 29^{\circ}\text{C}$, 1SD for data set population) (Supplementary material 1) should provide a minimum estimate of magma temperatures upon emplacement and are similar to the temperatures reported by Miller et al. (2003) for ‘cold’ and usually inheritance-rich granites. However, most studies indicate that granitoids should carry crystal fractions of $\sim 5 - 25\%$ from their source at temperatures of $\sim 750^{\circ}\text{C}$ (e.g. Miller et al. 1986; Patiño Douce and Beard, 1995; Patiño Douce and Harris, 1998; Miller, 2003). Harrison et al. (2007) suggested that zircon saturation temperatures may underestimate zircon crystallisation temperatures by up to 100°C , and may overestimate the proportions of inherited crystals transported from depth. Crucially, however, Annen et al. (2006a) have demonstrated that water activity may also play an important role in determining the crystal cargoes of ascending magmas. Calc-alkaline magmas generated in crustal hot zones are H_2O -rich, with higher pressures enabling large amounts of H_2O to remain dissolved. At $\sim 750^{\circ}\text{C}$ and moderate crustal depths of ~ 25 km, large volumes of granitic melt require ~ 6 wt% H_2O (Holtz and Johannes, 1994; Miller et al. 2003). Hot zone silicic magmas are therefore buoyant and have relatively low densities and viscosities even at low temperatures (Annen et al. 2006a). In consequence, such silicic magmas may readily segregate on timescales of 10^4 to 10^6 years by compaction (McKenzie, 1984; Jackson et al. 2003) or more rapidly under conditions of deformation (Brown, 1994; Petford, 2003). Subsequent silicic magma ascent from the hot zone may be rapid and adiabatic on timescales of hours or days (Clemens and Mawer, 1992; Petford, et al. 1993; Annen et al 2006a; Annen, et al. 2006b). During adiabatic ascent, granitic magmas may enter a super-liquidus state (Clemens et al. 1997; Annen et al. 2006a; Blundy and Cashman, 2001; Blundy et al. 2006;) due to the slightly steeper slope of the adiabat relative to the water-rich liquidus, resulting in the resorption of most or all entrained crystals (Fig. 11).

The abundance of hornblende in calc-alkaline magmas like those of the Criffell pluton suggests water saturated conditions (e.g. Berndt et al. 2005). Phase relations in silicic calc-alkaline dacites show that amphibole crystallisation requires water contents of $\sim 4 - 6$ wt % (Scaillet and Evans, 1999; Scaillet and MacDonald, 2001). These estimates further support the need for water contents of ~ 6 wt % for sufficient granitic melt generation at temperatures

of ~ 750°C (Holtz and Johannes, 1994; Miller et al. 2003). Assuming an H₂O content of ~ 6wt %, magmas that ascend along a 4°C/kbar adiabatic gradient (Holtz and Johannes, 1994) intersect the water-saturated liquidus at pressures of ~ 1kbar (~ 4 km) (Fig. 11). Crystallisation is likely to occur only after ascending magmas intersect the H₂O-saturated liquidus, leading to stalling, rapid loss of volatiles, increased viscosity and potentially rapid crystallisation (e.g. Blundy and Cashman, 2001; Blundy et al. 2006). Crystallisation depths of ~ 4 - 6 km indicated by amphibole barometry are therefore consistent with the stalling and crystallisation of magmas of granitic composition with ~ 6wt% H₂O at these depths due to intersection of the H₂O-saturated liquidus. In light of this, the absence of inherited zircons in cold granites (with temperatures of ~ 760°C) may need re-evaluation in terms of temperature (Miller et al. 2003) in addition to water contents and the potential effects of super-liquidus magmas.

It is thought that due to the potentially small volumes of single magma batches, the rapid water loss on intersecting the water-saturated liquidus and the subsequently large increases in viscosity, crystallisation is likely to occur under nearly closed system conditions (Annen et al. 2006a). This would be consistent with the preservation of near-liquidus compositions by some apatites (the most Ce-rich apatites) and the WR in metaluminous zones of the Criffell pluton (Fig. 8). Under such circumstances, mineral compositions, and particularly those of REE-rich accessory phases crystallising at shallow depths, will become highly susceptible to the competitive crystallisation of other co-existing accessory phases, as noted here. The resulting patterns of trace element concentrations in apatites and their host rocks may thus provide evidence of the ascent and crystallisation processes of magmas and the possible attainment of transient super-liquidus conditions during adiabatic ascent, prior to stalling and crystallisation. The passage of melts through a super-liquidus state ensures that open system deep crustal processes recorded by the WR remain distinct from closed system crystallisation processes recorded by the accessory and major minerals.

Confirmation of the processes associated with crustal hot zones and the assembly of multiple magma batches following melt separation and ascent to shallower levels indicate that pluton assembly is likely to have been incremental. Such assembly is consistent with a growing consensus that large plutonic bodies grow incrementally (Wiebe and Collins, 1998; Glazner et al. 2004; Coleman et al. 2004; Glazner and Bartley, 2006; Kemp et al. 2006b; Lipman,

2007; Miller, 2008; Appleby et al. 2008) and may explain how textural diversity occurs, often on short length scales, within large plutons such as Criffell.

Despite providing robust insights into magmatic processes, the trace element compositions of accessory minerals are in many situations likely to reflect processes that occur at shallow levels only. An integrated WR *and* accessory mineral approach is therefore needed to fully model the petrological history of silicic magmas that have likely followed protracted histories in lower and upper regions of the lithosphere. By contrast, the isotopic compositions of accessory minerals should retain evidence of processes that occurred prior to magma emplacement.

7. Concluding remarks

1. WR compositions in the Criffell pluton record the effects of open system differentiation (Stephens et al. 1985) in the deep crust. High WR $^{207}\text{Pb}/^{204}\text{Pb}$ isotope compositions (Thirlwall, 1989) indicate that the local Southern Uplands sedimentary rocks into which the Criffell pluton is emplaced were not the source of crustal contamination. More likely sources are found in Avalonian crust south of the Iapetus Suture, which is thought to extend to depths > 11 km beneath the Southern Uplands. Decreasing concentrations of Ce and Y in the WR can be modelled by assimilation of Avalonian sedimentary rocks and the fractional crystallisation of a mineral assemblage similar to that of mafic enclaves found in Criffell granodiorite.

2. Al-in-hornblende barometry and plagioclase-hornblende thermometry suggest that crystallisation of the present granodiorite crystal assemblage occurred at 0.8 - 1.5 kbars (~ 4 - 6 km depth) and ~ 680°C. Despite evidence for zircon saturation (progressively decreasing Zr with SiO₂ in the WR) and supracrustal contamination, the absence of inherited zircon indicates that the observed zircon assemblage crystallised on emplacement at shallower depths.

3. Accessory apatite inclusions in a range of host phases crystallised through bulk saturation of the magma. Variations of up to two orders-of-magnitude in the Ce and Y (trend 1) contents of apatites from single metaluminous samples result from the crystallisation of co-existing

allanite. Despite the importance of allanite in determining the composition of apatite in metaluminous samples, increasing LREE/HREE ratios with SiO₂ in the metaluminous WR suite suggest that, during WR differentiation, amphibole or zircon crystallisation (rather than allanite) was the dominant control on compositional evolution.

4. Apatites in peraluminous zones define a second trend of low Ce and Th together with elevated Y (and Yb) and have more negative WR-normalised Nd anomalies than those from metaluminous zones that are consistent with prior crystallisation of monazite. Evidence for monazite crystallisation is absent at the scale of even the most evolved WR samples, providing good evidence that the trace element trends defined by the WR suite and their apatite crystal cargoes were determined independently.

5. These results are consistent with the crustal hot zone model proposed by Annen and Sparks (2002) and Annen et al. (2006a), where WR compositions are determined by potentially large-scale, open system processes within nested sill complexes in the lower crust.

6. Small batches of water-rich (~ 6wt % H₂O), low-viscosity magma ascend from a deep crustal hot zone adiabatically and achieve a super-liquidus state, resorbing most or all of their crystal cargo, until they stall and crystallise at shallower depths of 4 to 6 km upon intersecting the water-saturated liquidus. It is at these shallower emplacement depths that crystallisation and textural maturation of the pluton occurs. The passage of melts through a super-liquidus state ensures that open system deep crustal processes recorded by the WR remain distinct from closed system crystallisation processes recorded by the accessory and major minerals.

7. Mainly closed system crystallisation within small melt volumes means that accessory apatite trace element compositions largely reflect the saturation of other, competing accessory minerals and that WR compositions are close to initial liquid compositions. Assembly of the Criffell pluton therefore appears to have been incremental.

8. Together, WR and accessory mineral data enable petrogenetic models to be developed at two very different scales and at high enough spatial and temporal resolution to enable processes of pluton assembly to be better assessed. The isotopic compositions retained by accessory minerals may faithfully record the effects of magma differentiation, despite not

having crystallised in regions where such compositions are determined. However, the trace element compositions of accessory minerals mainly reflect the crystallisation history at shallower levels. These physical and geochemical processes identified in the Criffell Pluton should be common to many metaluminous and peraluminous granitic plutons, and may be indicative of transient super-liquidus states of ascending silicic magmas.

REFERENCES CITED

Anderson JL, Smith DR (1995) The effects of temperature and fO_2 on the Al-in-hornblende barometer. *American Mineralogist* 80(5-6):549-559

Annen C, Blundy JD, Sparks RSJ (2006a) The genesis of intermediate and silicic magmas in deep crustal hot zones. *Journal of Petrology* 47(3):505-539

Annen C, Blundy JD, Sparks RSJ (2006b) The sources of granitic melt in Deep Hot Zones. *Transactions of the Royal Society of Edinburgh-Earth Sciences* 97:297-309

Annen C, Sparks RSJ (2002) Effects of repetitive emplacement of basaltic intrusions on thermal evolution and melt generation in the crust. *Earth and Planetary Science Letters* 203(3-4):937-955

Appleby SK, Graham CM, Gillespie MR, Hinton RW, Oliver GJH, Eimf (2008) A cryptic record of magma mixing in diorites revealed by high-precision SIMS oxygen isotope analysis of zircons. *Earth and Planetary Science Letters* 269(1-2):105-117

Atherton, M. P. & Ghani, A. A. (2002). Slab breakoff: a model for Caledonian, Late Granite syn-collisional magmatism in the orthotectonic (metamorphic) zone of Scotland and Donegal, Ireland. *Lithos* 62, 65-85.

Bacon CR (1983) Eruptive history of Mount Mazama and Crater Lake Caldera, Cascade Range, USA *Journal of Volcanology and Geothermal Research* 18(1-4):57-115

Bacon CR, Druitt TH (1988) Compositional evolution of the zoned calkalkaline magma chamber of Mount-Mazama, Crater Lake, Oregon *Contributions to Mineralogy and Petrology* 98(2):224-256

- 739
- 740 Bacon, C. R. (1989). Crystallisation of accessory phases in magmas by local saturation
 741 adjacent to phenocrysts. *Geochimica Et Cosmochimica Acta* **53**, 1055-1066.
- 742
- 743 Beamish D, Smythe DK (1986) Geophysical images of the deep crust: the Iapetus suture.
 744 *Journal of the Geological Society* 143:489-497
- 745
- 746 Belousova EA, Griffin WL, O'Reilly SY, Fisher NI (2002) Apatite as an indicator mineral for
 747 mineral exploration: trace-element compositions and their relationship to host rock type.
 748 *Journal of Geochemical Exploration* 76(1):45-69
- 749
- 750 Belousova EA, Walters S, Griffin WL, O'Reilly SY (2001) Trace-element signatures of
 751 apatites in granitoids from the Mt Isa Inlier, northwestern Queensland. *Australian Journal of*
 752 *Earth Sciences* 48(4):603-619
- 753
- 754 Berndt J, Koepke J, Holtz F (2005) An experimental investigation of the influence of water
 755 and oxygen fugacity on differentiation of MORB at 200 MPa. *Journal of Petrology*
 756 46(1):135-167
- 757
- 758 Blatter DL, Carmichael ISE (1998) Plagioclase-free andesites from Zitacuaro (Michoacan),
 759 Mexico: petrology and experimental constraints. *Contributions to Mineralogy and Petrology*
 760 132(2):121-138
- 761
- 762 Blundy J, Cashman K (2001) Ascent-driven crystallisation of dacite magmas at Mount St
 763 Helens, 1980-1986. *Contributions to Mineralogy and Petrology* 140(6):631-650
- 764
- 765 Blundy J, Cashman K (2005) Rapid decompression-driven crystallization recorded by melt
 766 inclusions from Mount St. Helens volcano. *Geology* 33(10):793-796
- 767
- 768 Blundy J, Cashman K, Humphreys M (2006) Magma heating by decompression-driven
 769 crystallization beneath andesite volcanoes. *Nature* 443(7107):76-80
- 770
- 771 Blundy JD, Holland TJB (1990) Calcic amphibole equilibria and a new amphibole-
 772 plagioclase geothermometer. *Contributions to Mineralogy and Petrology* 104(2):208-224

- 773
- 1
2 774 Bowen NL (1928) The evolution of igneous rocks, vol. Princeton University Press, p 334
- 3
4 775
- 5 776 Bradley DC (2011) Secular trends in the geologic record and the supercontinent cycle. Earth-
6
7 777 Science Reviews 108(1-2):16-33
8
9 778
- 10 779 Brown M (1994) The Generation, Segregation, Ascent and Emplacement of Granite Magma
11
12 780 – the Migmatite-to Crustally-Derived- Granite Connection in Thickened Orogens. Earth-
13
14 781 Science Reviews 36(1-2):83-130
15
16 782
- 17 783 Brown PE, Ryan PD, Soper NJ, Woodcock NH (2008) The Newer Granite problem revisited:
18
19 784 a transtensional origin for the Early Devonian Trans-Suture Suite. Geological Magazine
20
21 785 145(2):235-256
22
23 786
- 24 787 Chappell BW, White AJR, Williams IS, Wyborn D (2004) Low- and high-temperature
25
26 788 granites. Transactions of the Royal Society of Edinburgh-Earth Sciences 95:125-140
27
28 789
- 29 790 Chu MF, Wang KL, Griffin WL, Chung SL, O'Reilly SY, Pearson NJ, Iizuka Y (2009)
30
31 791 Apatite Composition: Tracing Petrogenetic Processes in Transhimalayan Granitoids. Journal
32
33 792 of Petrology 50(10):1829-1855
34
35 793
- 36 794 Claiborne LL, Miller CF, Wooden JL (2010) Trace element composition of igneous zircon: a
37
38 795 thermal and compositional record of the accumulation and evolution of a large silicic
39
40 796 batholith, Spirit Mountain, Nevada. Contributions to Mineralogy and Petrology 160(4):511-
41
42 797 531
43
44 798
- 45 799 Clemens JD, Mawer CK (1992) Granitic Magma Transport by Fracture Propagation.
46
47 800 Tectonophysics 204(3-4):339-360
48
49 801
- 50 802 Clemens JD, Petford N, C.K M (1997) Ascent mechanisms of granitic magmas: cause and
51
52 803 consequence. In: Holness M (ed) Deformation-Enhanced Fluid Transport in the Earth's Crust
53
54 804 and Mantle, vol. Chapman & Hall, London, pp 145-172
55
56 805
57
58
59
60
61
62
63
64
65

- 806 Coleman DS, Gray W, Glazner AF (2004) Rethinking the emplacement and evolution of
807 zoned plutons: Geochronologic evidence for incremental assembly of the Tuolumne Intrusive
808 Suite, California. *Geology* 32(5):433-436
809
- 810 Cooper DC, Lee MK, Fortey NJ, Cooper AH, Rundle CC, Webb BC, Allen PM (1988) The
811 Crummock Water aureole: a zone of metasomatism and source of ore metals in the English
812 Lake District. *Journal of the Geological Society* 145:523-540
813
- 814 Costa F, Scaillet B, Pichavant M (2004) Petrological and experimental constraints on the pre-
815 eruption conditions of Holocene dacite from Volcan San Pedro (36 degrees S, Chilean
816 Andes) and the importance of sulphur in silicic subduction-related magmas. *Journal of*
817 *Petrology* 45(4):855-881
818
- 819 Couch S, Harford CL, Sparks RSJ, Carroll MR (2003) Experimental constraints on the
820 conditions of formation of highly calcic plagioclase microlites at the Soufriere Hills Volcano,
821 Montserrat. *Journal of Petrology* 44(8):1455-1475
822
- 823 Courrioux G (1987) Oblique diapirism - The Criffel granodiorite granite zoned pluton
824 (Southwest Scotland) *Journal of Structural Geology* 9(3):313-330
825
- 826 Debari, S. M. & Coleman, R. G. (1989). Examination of the deep levels of an island arc:
827 Evidence from the Tonsina Ultramafic-Mafic Assemblage, Tonsina, Alaska. *Journal of*
828 *Geophysical Research-Solid Earth and Planets* **94**, 4373-4391.
829
- 830 DePaolo DJ (1981) Trace element and isotopic effects of combined wallrock assimilation and
831 fractional crystallization. *Earth and Planetary Science Letters* 53(2):189-202
832
- 833 Druitt TH, Bacon CR (1989) Petrology of the zoned calcalkaline magma chamber of Mount
834 Mazama, Crater Lake, Oregon. *Contributions to Mineralogy and Petrology* 101(2):245-259
835
- 836 Eiler JM (2007) *Geology - On the origins of granites.* *Science* 315(5814):951-952
837 Ewart A, Griffin WL (1994) Application of proton-microprobe data to trace-element
838 partitioning in volcanic-rocks. *Chemical Geology* 117(1-4):251-284
839

840 Ewart, A. & Griffin, W. L. (1994). Application of proton-microprobe data to trace-element
841 partitioning in volcanic-rocks. *Chemical Geology* **117**, 251-284
842
843 Freeman B, Klemperer SL, Hobbs RW (1988) The deep structure of Northern England and
844 the Iapetus Suture Zone from BIRPS deep seismic reflection profiles Journal of the Geological
845 Society 145:727-&
846
847 Fujimaki H (1986) Partition-coefficients of Hf, Zr, and REE between zircon, apatite, and
848 liquid. Contributions to Mineralogy and Petrology 94(1):42-45
849
850 Fujimaki H, Tatsumoto M, K. A (1984) Partition coefficients of Hf, Zr, and REE between
851 phenocrysts and groundmasses. Journal of Geophysical Research 89:662-672
852
853 Gardner JE, Carey S, Sigurdsson H, Rutherford MJ (1995) Influence of magma composition
854 on the eruptive activity of Mount St. Helens, Washington. Geology 23(6):523-526
855
856 Glazner AF, Bartley JM (2006) Is stopping a volumetrically significant pluton emplacement
857 process? Geological Society of America Bulletin 118(9-10):1185-1195
858
859 Glazner AF, Bartley JM, Coleman DS, Gray W, Taylor RZ (2004) Are plutons assembled
860 over millions of years by amalgamation from small magma chambers? GSA Today 14(4-11)
861
862 Hall J, Brewer, J.A, Matthews, D.H, Warner, M.R (1984) Crustal structure across the
863 Caledonides from the 'WINCH' seismic reflection profile: Influences on the evolution of the
864 Midland Valley of Scot. Transactions of the Royal Society of Edinburgh-Earth Sciences
865 75:97-109
866
867 Halliday AN (1984) Coupled Sm-Nd and U-Pb Systematics in Late Caledonian Granites and
868 the Basement under Northern Britain. Nature 307(5948):229-233
869
870 Halliday AN, Stephens WE, Harmon RS (1980) Rb-Sr and O Isotopic Relationships in 3
871 Zoned Caledonian Granitic Plutons, Southern Uplands, Scotland - Evidence for Varied
872 Sources and Hybridization of Magmas. Journal of the Geological Society 137(MAY):329-
873 348

874

875 Harford CL, Pringle MS, Sparks RSJ, Young SR (2002) The volcanic evolution of
876 Montserrat using $^{40}\text{Ar}/^{39}\text{Ar}$ geochronology In: Druitt TH, Kokelaar BP (eds) The Eruption
877 of Soufriere Hills Volcano, Montserrat (1995 to 1999), vol 21. Geological Society, London
878 Memoirs, pp 93-113

879

880 Harmon, R. S. & Halliday, A. N. (1980). Oxygen and strontium isotope relationships in the
881 British Caledonian granites *Nature* **283**, 21-25.

882

883 Harmon, R. S., Halliday, A. N., Clayburn, J. A. P. & Stephens, W. E. (1984). Chemical and
884 isotopic systematics of the Caledonian intrusions of Scotland and Northern England - A guide
885 to magma source regions and magma crust interaction. *Philosophical Transactions of the*
886 *Royal Society of London Series a-Mathematical Physical and Engineering Sciences* **310**, 709-
887 742.

888

889 Harrison TM, Watson EB, Aikman AB (2007) Temperature spectra of zircon crystallization
890 in plutonic rocks. *Geology* 35(7):635-638

891

892 Hawkesworth CJ, Dhuime B, Pietranik AB, Cawood PA, Kemp AIS, Storey CD (2010) The
893 generation and evolution of the continental crust. *Journal of the Geological Society*
894 167(2):229-248

895

896 Higgins, M. D. & Roberge, J. (2003). Crystal size distribution of plagioclase and amphibole
897 from Soufrière Hills Volcano, Monserrat: evidence for dynamic crystallization–textural
898 coarsening cycles. *Journal of Petrology* **44**, 1401-1411.

899

900 Highton A (1999) Late Silurian and Devonian granitic intrusions of Scotland. In: Stephenson
901 D, Bevins, RE, Millward, D, Highton, AJ, Parsons, I, Stone, P, Wadsworth, WJ (ed)
902 Caledonian Igneous Rocks of Britain, vol Geological Conservation Review Series: Joint
903 Nature Conservation Committee. pp 397-404

904

905 Holden P, Halliday AN, Stephens WE (1987) Neodymium and Strontium Isotope Content of
906 Microdiorite Enclaves Points to Mantle Input to Granitoid Production. *Nature* 330(6143):53-
907 56

- 908
- 1
2 909 Holden PH, A. N. ; Stephens., W. E. ; Henny., P. J. (1991) Chemical and isotopic evidence
3
4 910 for major mass transfer between mafic enclaves and felsic magma. *Chemical Geology*
5 911 92:135-152
6
7 912
- 8
9 913 Holtz F, Becker A, Freise M, Johannes W (2001) The water-undersaturated and dry Qz-Ab-
10
11 914 Or system revisited. Experimental results at very low water activities and geological
12
13 915 implications. *Contributions to Mineralogy and Petrology* 141(3):347-357
14
15 916
- 16 917 Holtz F, Johannes W (1994) Maximum and minimum water contents of granitic melts:
17
18 918 Implications for chemical and physical properties of ascending magmas. *Lithos* 32(1-2):149-
19
20 919 159
21
22 920
- 23 921 Hoskin PWO, Kinny PD, Wyborn D, Chappell BW (2000) Identifying accessory mineral
24
25 922 saturation during differentiation in granitoid magmas: an integrated approach. *Journal of*
26
27 923 *Petrology* 41(9):1365-1396
28
29 924
- 30
31 925 Jackson MD, Cheadle MJ, Atherton MP (2003) Quantitative modeling of granitic melt
32
33 926 generation and segregation in the continental crust. *Journal of Geophysical Research-Solid*
34
35 927 *Earth* 108(B7)
36
37 928
- 38 929 Janots E, Brunet F, Goffe B, Poinssot C, Burchard M, Cemic L (2007) Thermochemistry of
39
40 930 monazite-(La) and dissakisite-(La): Implications for monazite and allanite stability in
41
42 931 metapelites. *Contributions to Mineralogy and Petrology* 154(1):1-14
43
44 932
- 45 933 Johnson MC, Rutherford MJ (1989) Experimental calibration of the aluminum-in-hornblende
46
47 934 geobarometer with application to Long Valley caldera (California) volcanic rocks *Geology*
48
49 935 17(9):837-841
50
51 936
- 52
53 937 Jull M, Kelemen PB (2001) On the conditions for lower crustal convective instability. *Journal*
54
55 938 *of Geophysical Research-Solid Earth* 106(B4):6423-6446
56
57 939
- 58 940 Kay, R. W. & Kay, S. M. (1993). Delamination and delamination magmatism.
59
60 941 *Tectonophysics* **219**, 177-189.
61

- 942
- 943 Kemp AIS, Hawkesworth CJ, Foster GL, Paterson BA, Woodhead JD, Hergt JM, Gray CM,
 944 Whitehouse MJ (2007) Magmatic and crustal differentiation history of granitic rocks from
 945 Hf-O isotopes in zircon. *Science* 315(5814):980-983
 946
- 947 Kemp AIS, Hawkesworth CJ, Paterson BA, Foster GL, Kinny PD, Whitehouse MJ, Maas R,
 948 Eimf (2006a) Exploring the plutonic-volcanic link: a zircon U-Pb, Lu-Hf and O isotope study
 949 of paired volcanic and granitic units from southeastern Australia. *Transactions of the Royal
 950 Society of Edinburgh-Earth Sciences* 97:337-355
 951
- 952 Kemp AIS, Hawkesworth CJ, Paterson BA, Kinny PD (2006b) Episodic growth of the
 953 Gondwana supercontinent from hafnium and oxygen isotopes in zircon. *Nature*
 954 439(7076):580-583
 955
- 956 Klemperer SL, Matthews DH (1987) Iapetus Suture Located beneath the North-Sea by Birps
 957 Deep Seismic-Reflection Profiling. *Geology* 15(3):195-198
 958
- 959 Klemperer SL, Ryan PD, Snyder DB (1991) A deep seismic-reflection transect across the
 960 Irish Caledonides *Journal of the Geological Society* 148:149-&
 961
- 962 Klimm K, Blundy JD, Green TH (2008) Trace element partitioning and accessory phase
 963 saturation during H₂O-saturated melting of basalt with implications for subduction zone
 964 chemical fluxes. *Journal of Petrology* 49(3):523-553
 965
- 966 Lipman PW (2007) Incremental assembly and prolonged consolidation of Cordilleran magma
 967 chambers: Evidence from the Southern Rocky Mountain volcanic field. *Geosphere* 3(1):42-
 968 70
 969
- 970 London, D. (1992). Phosphorus in S-type magmas: the P₂O₅ content of feldspars from
 971 peraluminous granites, pegmatites, and rhyolites. *American Mineralogist* 77, 126-145.
 972
- 973 Mahood G, Hildreth W (1983) An experimental study of the partitioning of copper between
 974 pyrrhotite and a high-silica rhyolitic melt. *Geochimica Et Cosmochimica Acta* 47(1):11-30
 975

- 976 Martel C, Pichavant M, Holtz F, Scaillet B, Bourdier J-L, Traineau H (1999) Effects of fO_2
977 and H_2O on andesite phase relations between 2 and 4 kbar. Journal of Geophysical Research
978 104:29453-29470
979
- 980 McKenzie D (1984) The Generation and Compaction of Partially Molten Rock. Journal of
981 Petrology 25(3):713-765
982
- 983 Miller CF, McDowell SM, Mapes RW (2003) Hot and cold granites? Implications of zircon
984 saturation temperatures and preservation of inheritance. Geology 31(6):529-532
985
- 986 Miller CF, Rapp RP, Watson EB (1986) AFM mineral-felsic liquid phase relations: Potential
987 for elucidation of the origin and evolution of felsic magmas. Geological Society of America
988 Abstracts with Programs 18(6):695
989
- 990 Miller JS (2008) Assembling a pluton... one increment at a time. Geology 36(6):511-512
991
- 992 Montel JM (1986) Experimental determination of the solubility of Ce-monazite in SiO_2 -
993 Al_2O_3 - K_2O - Na_2O melts at 800°C, 2 kbar, under H_2O -saturated conditions Geology
994 14(8):659-662
995
- 996 Moore G, Carmichael ISE (1998) The hydrous phase equilibria (to 3 kbar) of an andesite and
997 basaltic andesite from western Mexico: constraints on water content and conditions of
998 phenocryst growth. Contributions to Mineralogy and Petrology 130(3-4):304-319
999
- 1000 Muntener O, Kelemen PB, Grove TL (2001) The role of H_2O during crystallization of
1001 primitive arc magmas under uppermost mantle conditions and genesis of igneous
1002 pyroxenites: an experimental study. Contributions to Mineralogy and Petrology 141(6):643-
1003 658
1004
- 1005 Nash, W. P. (1984). *Phosphate minerals in terrestrial igneous and metamorphic rocks*.
1006 Berlin: Springer-Verlag.
1007

- Neilson, J. C., Kokelaar, B. P. & Crowley, Q. G. (2009). Timing, relations and cause of plutonic and volcanic activity of the Siluro-Devonian post-collision magmatic episode in the Grampian Terrane, Scotland. *Journal of the Geological Society* **166**, 545-561
- Oliver, G. J. H., Wilde, S. A. & Wan, Y. (2008). Geochronology and geodynamics of Scottish granitoids from the late Neoproterozoic break-up of Rodinia to Palaeozoic collision. *Journal of the Geological Society* **165**, 661-674
- Patiño Douce AE, Beard JS (1995) Dehydration-melting of Biotite Gneiss and Quartz Amphibolite from 3 to 15 kbar. *Journal of Petrology* 36(3):707-738
- Patiño Douce AE, Harris N (1998) Experimental constraints on Himalayan anatexis. *Journal of Petrology* 39(689-710)
- Petford N (2003) Rheology of granitic magmas during ascent and emplacement. *Annual Review of Earth and Planetary Sciences* 31:399-427
- Petford N, Kerr RC, Lister JR (1993) Dike Transport of Granitoid Magmas. *Geology* 21(9):845-848
- Pidgeon RT, Aftalion M (1978) Cogenetic and inherited zircon U-Pb systems in granites: Palaeozoic granites of Scotland and England, in Bowes, D.R., Leake, B.E., Crustal evolution in northwestern Britain and adjacent regions. *Geological Journal Special Issue*:183-220
- Prouteau G, Scaillet B (2003) Experimental constraints on the origin of the 1991 Pinatubo dacite. *Journal of Petrology* 44(12):2203-2241
- Prowatke S, Klemme S (2006) Trace element partitioning between apatite and silicate melts. *Geochimica Et Cosmochimica Acta* 70(17):4513-4527
- Roberts N (2012) Increased loss of continental crust during supercontinent amalgamation. *Gondwana Research* 21(994-1000)

- Rutherford MJ, Devine JD (2003) Magmatic conditions and magma ascent as indicated by hornblende phase equilibria and reactions in the 1995-2002 Soufriere Hills magma. *Journal of Petrology* 44(8):1433-1454
- Sano Y, Terada K, Fukuoka T (2002) High mass resolution ion microprobe analysis of rare earth elements in silicate glass, apatite and zircon: lack of matrix dependency. *Chemical Geology* 184(3-4):217-230
- Scailliet B, Evans BW (1999) The 15 June 1991 eruption of Mount Pinatubo. I. Phase equilibria and pre-eruption P-T-fO(2)-fH(2)O conditions of the dacite magma. *Journal of Petrology* 40(3):381-411
- Scailliet B, MacDonald R (2001) Phase relations of peralkaline silicic magmas and petrogenetic implications. *Journal of Petrology* 42(4):825-845
- Schnetzler CC, Philpott JA (1970) Partition coefficients of rare-earth elements between igneous matrix material and rock-forming mineral phenocrysts 2. *Geochimica Et Cosmochimica Acta* 34(3):331-&
- Sha LK, Chappell BW (1999) Apatite chemical composition, determined by electron microprobe and laser-ablation inductively coupled plasma mass spectrometry, as a probe into granite petrogenesis. *Geochimica Et Cosmochimica Acta* 63(22):3861-3881
- Shnukov SE, Cheburkin AK, Andreev AV (1989) Geochemistry of wide-spread coexisting accessory minerals and their role in investigation of endogenic and exogenic processes. *Geological Journal* 2:107-114
- Sisson TW (1994) Hornblende-Melt Trace-Element Partitioning Measured by Ion Microprobe. *Chemical Geology* 117(1-4):331-344
- Soper NJ, Woodcock NH (2003) The lost Lower Old Red Sandstone of England and Wales: a record of post-Iapetan flexure or Early Devonian transtension? *Geological Magazine* 140(6):627-647

- Stephens WE (1988) Granitoid plutonism in the Caledonian orogen of Europe. In: Harris A, Fettes, DJ (ed) *The Caledonian-Appalachian Orogen*, vol 38. Geological Society of London, Special Publication, pp 389-403
- Stephens WE (1992) Spatial, Compositional and Rheological Constraints on the Origin of Zoning in the Criffell Pluton, Scotland. *Transactions of the Royal Society of Edinburgh-Earth Sciences* 83:191-199
- Stephens WE, Halliday AN (1980) Discontinuities in the Composition Surface of a Zoned Pluton, Criffell, Scotland. *Geological Society of America Bulletin* 91(3):165-170
- Stephens WE, Whitley JE, Thirlwall MF, Halliday AN (1985) The Criffell zoned pluton: correlated behaviour of rare earth element abundances with isotopic systems. *Contributions to Mineralogy and Petrology* 89:226-238
- Stephens, W. E. (1999). Late Silurian and Devonian granitic intrusions of Scotland. In: Stephenson, D., Bevins, RE, Millward, D, Highton, AJ, Parsons, I, Stone, P, Wadsworth, WJ (ed.) *Caledonian Igneous Rocks of Britain*, 456-460.
- Stone, P. & Evans, J. A. (1995). Nd-isotope study of provenance patterns across the Iapetus Suture. *Geological Magazine* **132**, 571-580.
- Stone P, Evans JA (1997) A comparison of the Skiddaw and Manx groups (English Lake District and Isle of Man) using neodymium isotopes. *Proceedings of the Yorkshire Geological Society* 51:343-347
- Thirlwall, M. F. (1986). Lead isotope evidence for the nature of the mantle beneath Caledonian Scotland *Earth and Planetary Science Letters* **80**, 55-70.
- Thirlwall MF (1989) Movement on proposed tectonic boundaries in northern Britain: constraints from Ordovician-Devonian igneous rocks *Journal of the Geological Society, London* 146:373-376

- Thomas, L. J., Harmon, R.S., Oliver, G.J.H. (1985). Stable isotope composition of alteration fluids in low-grade Lower Palaeozoic Rocks, English Lake District. *Mineralogical Magazine* **49**.
- Thomas JB, Bodnar RJ, Shimizu N, Sinha AK (2002) Determination of zircon/melt trace element partition coefficients from SIMS analysis of melt inclusions in zircon. *Geochimica Et Cosmochimica Acta* 66(16):2887-2901
- Tiepolo M, Oberti R, R V (2002) Trace-element incorporation in titanite: constraints from experimentally determined solid/liquid partition coefficients. *Chemical Geology* 191:105-119
- Ulmer P (2007) Differentiation of mantle-derived calc-alkaline magmas at mid to lower crustal levels: experimental and petrologic constraints. *Periodico di Mineralogia* 76:309-325
- Waters JW (1909) Radioactive minerals in common rocks. *Philosophical Magazine* 18:677-679
- Watson EB, Harrison TM (1983) Zircon saturation revisited: Temperature and composition effects in a variety of crustal magma types. *Earth and Planetary Science Letters* 64:295-304
- Wiebe RA, Collins WJ (1998) Depositional features and stratigraphic sections in granitic plutons: implications for the emplacement and crystallization of granitic magma. *Journal of Structural Geology* 20(9-10):1273-1289
- Zindler, A. & Hart, S. (1986). Chemical Geodynamics. *Annual Review of Earth and Planetary Sciences* **14**, 493-571.

ACKNOWLEDGEMENTS

Funding was provided by a NERC CASE Studentship and a BGS BUFI grant. We are also grateful to NERC for use of the Edinburgh Ion Microprobe Facility and in particular to John Craven for his support and expertise. Chris Hayward is thanked for help with electron microprobe analyses and Mike Hall for support with preparation of zircon mounts and thin sections. Angus Calder and Donald Herd provided help with mineral separation at the University of St Andrews. We are indebted to Ed Stephens (University of St Andrews) for advice prior to fieldwork and during subsequent data analysis. Discussions with Godfrey

Fitton and Nigel Harris together with helpful reviews by two anonymous reviewers have further developed and significantly improved the manuscript. We thank Jon Blundy for careful and constructive comments and editing.

FIGURES

Fig. 1 Map of the Criffell pluton. Paler shading reflects increasing WR SiO₂. Zone mineralogy is as follows: 1) clinopyroxene-biotite-hornblende granodiorite; 2) biotite-hornblende granodiorite; 3) biotite granite; 4) biotite-muscovite granite 5) muscovite-biotite granite. Minerals listed in order of increasing modal abundance (Stephens et al. 1985). Black points denote sample sites. Inset: Regional map of major Scottish plutons. Abbreviations are as follows: HBF – Highland Boundary Fault, IS – Iapetus Suture.

Fig. 2a) Petrographic relations between phases in the outer zones (Zone 1) of the Criffell pluton. b) Petrographic relations in Zone 4. Images *a* and *b* show the euhedral nature of apatite inclusions in different host phases. c) Cathodoluminescence (CL) image of a zoned zircon with apatite inclusion from Zone 1. d) CL image of a zoned zircon crystal with apatite inclusion from Zone 3. Abbreviations: Ap – apatite, Bt – biotite, Hb – hornblende, K-Spar – potassium feldspar, Plag – plagioclase feldspar, Qtz – quartz, Sp – sphene, Zrc – zircon.

Fig. 3 Pb-Pb diagram modified from Thirlwall (1989) showing the Pb isotope compositions of the TSS plutons, Skiddaw Group sediments (Thomas 1985; Stone and Evans 1997), Southern Uplands sediments (Stone and Evans 1995), Borrowdale Volcanic Group (BVG) (Thirlwall, 1986) and depleted mantle (Zindler and Hart, 1986). All plutons extend to more radiogenic ²⁰⁷Pb/²⁰⁴Pb compositions than the Southern Uplands sediments into which they are intruded. Numbers in brackets refer to the number of available analyses.

Fig. 4 Harker plots showing a selection of major and trace elements vs. SiO₂ for whole-rock samples from the Criffell pluton distinguished by mineralogical zone (see figure key). Major element data are presented as oxide wt %; trace elements are presented as ppm. Data from this study and Stephens and Halliday (1980) (see Supplementary material 1).

Fig. 5 Ce-Y data for the WR suite and apatite crystals from single samples (see figure key). The WR compositions of samples used for apatite analyses are plotted using stars labeled

with their zone number. Substantial variability is seen in the compositions of apatite crystals from single samples, similar in percentage terms to that of the entire WR suite. Inset figure shows WR data and three petrological models: assimilation and fractional crystallisation (AFC), fractional crystallisation (FC) and simple mass balance mixing. In all models, granodiorite sample 244 from Stephens et al. (1985) has been used as a starting composition (Ce = 98 ppm, Y = 13 ppm). For AFC modeling, Skiddaw Group sedimentary rocks have been used as a crustal contaminant (Ce = 35 ppm, Y = 86 ppm, from Cooper et al. 1988) and assimilation to fractional crystallisation ratio of 0.3 assumed based on a similar study by Stephens et al. (1985). A crystal assemblage similar to that of mafic enclaves found in granodiorites has been used with modal proportions of: plagioclase = 40%, amphibole = 35%, biotite = 20%, sphene = 2.5%, apatite = 2% and zircon = 0.5%). Partition coefficients have been taken or estimated from Fujimaki et al. (1984), Ewart and Griffin (1994), Sisson (1994), Schnetzler and Philpott (1970), Tiepolo et al. (2002), Sano et al. (2002), Thomas et al. (2002), Fujimaki et al. (1986) and Prowatke and Klemme (2006). Mass balance has been used to model simple mixing between granodiorite sample 244 and Skiddaw Group sedimentary rock. AFC models provide the closest match with WR analyses

Fig. 6 Chondrite-normalised REE patterns for apatites in different zones of the Criffell pluton. Apatite hosted by zircon in Zone 3 is distinguished (red, dashed lines) from that hosted by other phases and shares more characteristics with those in zones 1 and 2. Apatite hosted by other phases in Zone 3 is similar to that in Zone 5.

Fig. 7 Ce (ppm) vs. Y (ppm) in apatites from zones 1 to 5 of the Criffell pluton. Apatite from zones 1 and 2 (a) define near vertical trends characterised by Ce depletion. Apatite from zones 4 and 5 (c) define a near-horizontal trend of Y depletion and consistently low Ce. The compositions of a small number of apatite crystals from Zone 3 (b) resemble those of apatite crystals from metaluminous zones 1 and 2. The majority of apatite in Zone 3 resemble those in zones 4 and 5, but shows a more pronounced trend of Ce depletion. 2 SD analytical error bars are shown for EPMA analyses. Ion probe analyses are subject to smaller errors (~ 10%). (d) is a schematic illustration of compositional trends in metaluminous and peraluminous samples. The former is controlled primarily by allanite extraction, the latter is inferred to reflect initial LREE depletion and HREE enrichment caused by early monazite crystallisation. Later-crystallised apatite follows a trend of HREE depletion.

Fig. 8 Calculated melt compositions. Ce and Yb melt compositions calculated from apatite compositions (small circles) using published apatite-melt partition coefficients (Fujimaki 1986). Yb data are only available for ion probe analyses. Average whole-rock (WR) compositions for each zone (red stars) were calculated using data from Stephens and Halliday (1980) and Stephens et al. (1985) with 1SD error bars shown for each population (zone). (a) and (c) also show calculated crystallisation models assuming a starting composition similar to average WR for Zone 1. The minerals used and their modal proportions are listed in the figure. Peraluminous crystallisation models assume a starting composition that post-dates monazite saturation (Yb = 9 ppm, Ce = 50 ppm). Shaded fields show the Ce-Yb compositions of the entire WR suite.

Fig. 9a) Apatite Ce vs. Th (ppm) for all zones of the Criffell pluton. R^2 values are listed in the key and reflect the extent to which Th and Ce correlate. Positive correlations are observed in metaluminous zones only and relate to simultaneous crystallisation of allanite. Low concentrations of Th in peraluminous zones reflect earlier monazite crystallisation, while low R^2 values indicate little further depletion of Th with Ce and monazite crystallisation. b) Apatite Y vs. Th showing similar results to the previous plot. R^2 values for Y-Th correlations for each zone are given in the key.

Fig. 10 Calculated apatite Nd anomalies normalised to average WR Nd anomalies for different zones [$Nd/Nd^* = Nd/(Ce \times Sm)^{1/2}$]. WR REE data from Stephens et al. (1985). A general decrease from zones 1 to 5 is apparent in WR-normalised Nd anomalies in apatites from progressively more evolved zones and cannot have been inherited from the WR. Negative Nd anomalies reflect saturation of monazite.

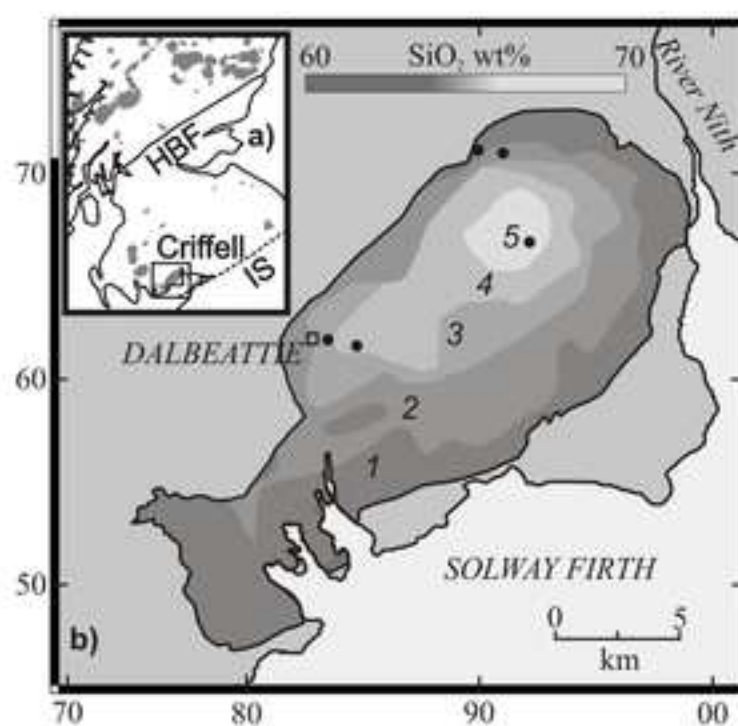
Fig. 11 Pressure-temperature diagram showing the adiabatic ascent of a granitic magma generated at ~ 7 kbar and ~ 750°C with a water content of ~ 6 wt % (stage I). Small ticks indicate intersection points between liquidus with different water contents and the water-saturated liquidus. Different processes are shown to take place at different stages of ascent (after Annen et al. 2006a). The positions of water-rich and water-saturated granitic liquidus are taken from Holtz et al. (2001). The melt is assumed to ascend adiabatically with a cooling of 4°C/kbar (Holtz and Johannes, 1994) (stage II). Following segregation from the melt zone, the melt temperature exceeds that of the liquidus, leading to a super-liquidus state (Clemens et al. 1997) and the likely resorption of entrained crystals. Water saturation is reached at ~ 2

1244 kbars at a temperature that is higher than that of the liquidus (stage III). Crystallisation and
1245 degassing should occur upon intersection with the water saturated liquidus (stage IV) at ~
1246 1kbar and ~730°C.

1247
1248
1249

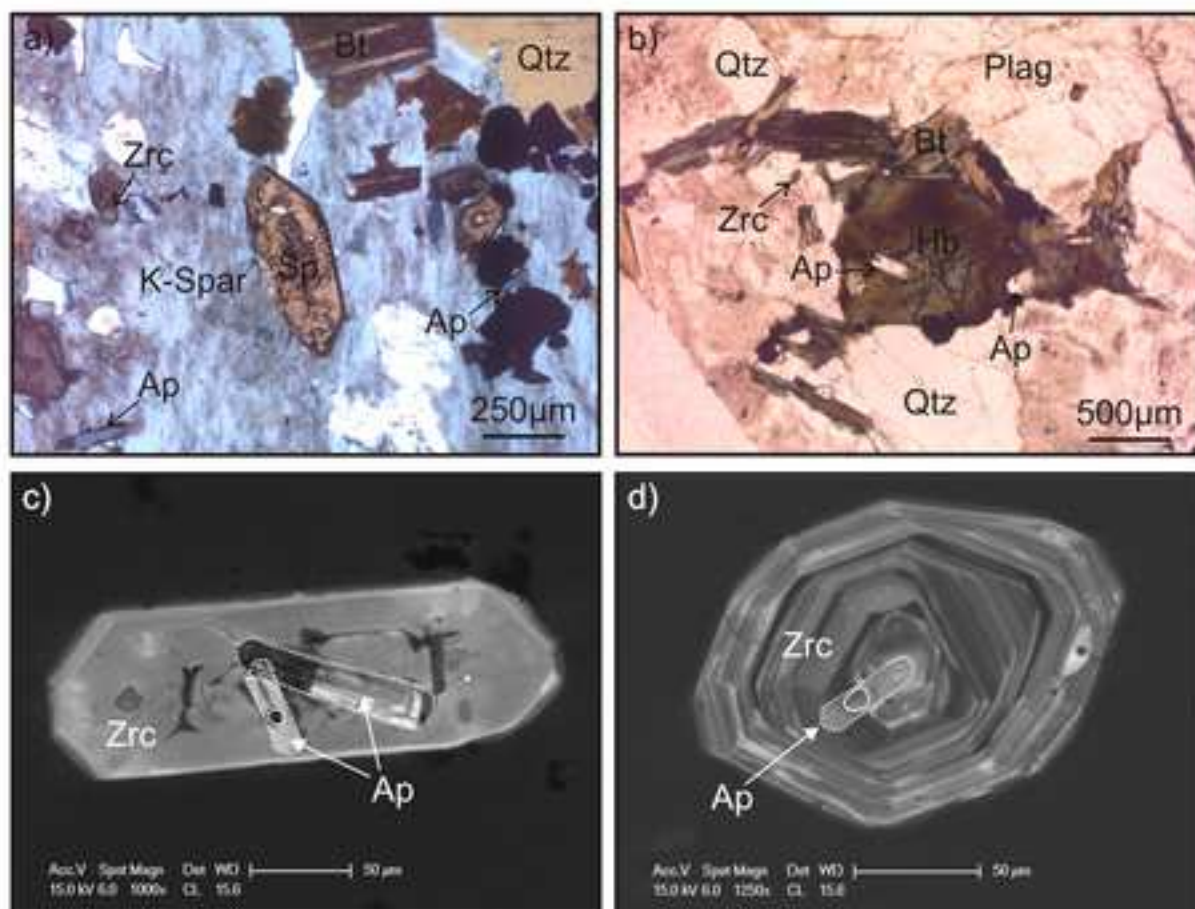
10
11
12
13
14
15
16
17
18
19
20
21
22
23
24
25
26
27
28
29
30
31
32
33
34
35
36
37
38
39
40
41
42
43
44
45
46
47
48
49
50
51
52
53
54
55
56
57
58
59
60
61
62
63
64
65

Figure. 1



Author name: Andrew Miles
Figure number: 1
File Extension: Figure_1.pdf

Figure 2



Author name: Andrew Miles

Figure number: 2

File Extension: Figure_2.pdf

Figure 3

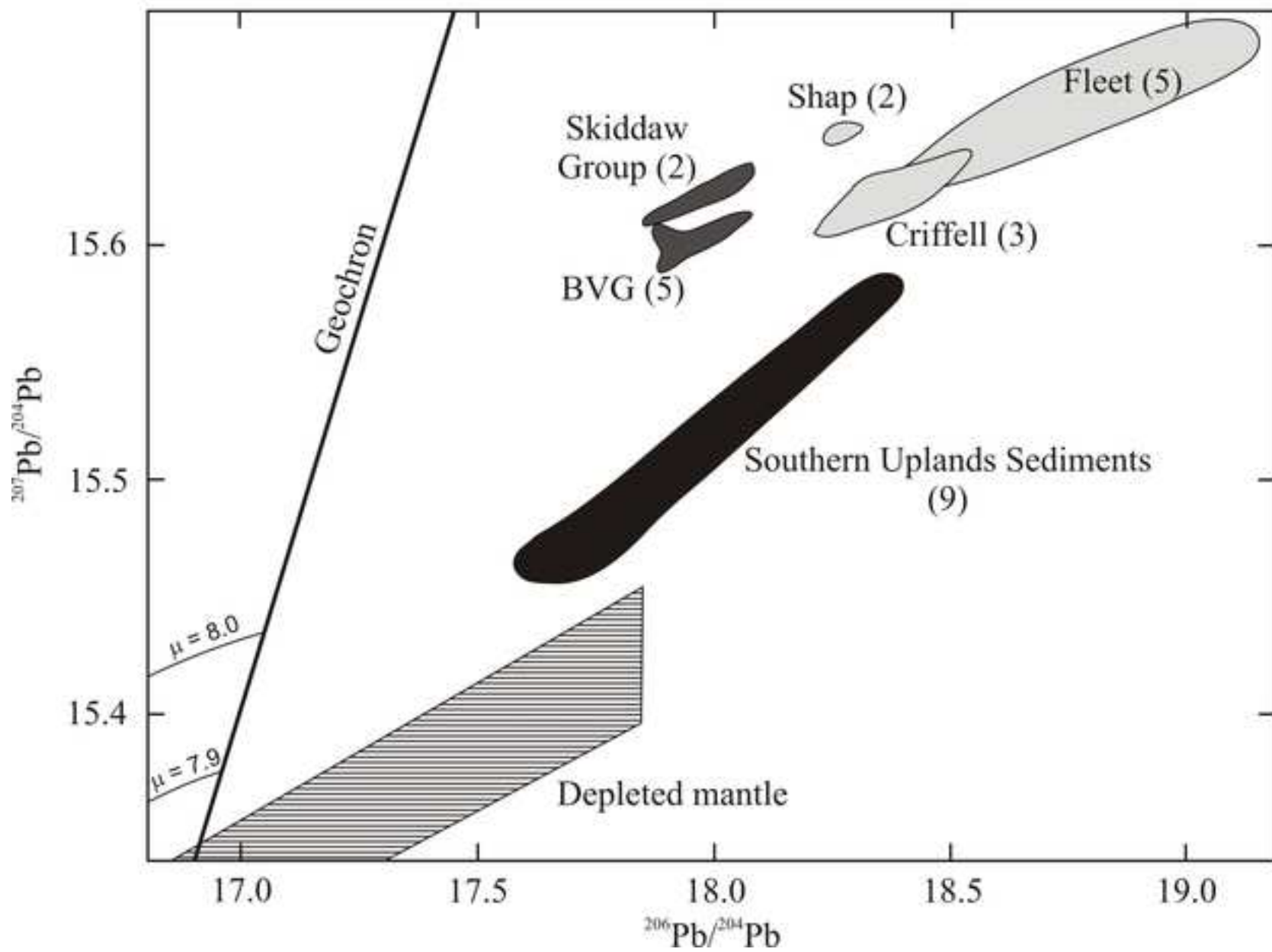


Figure 4

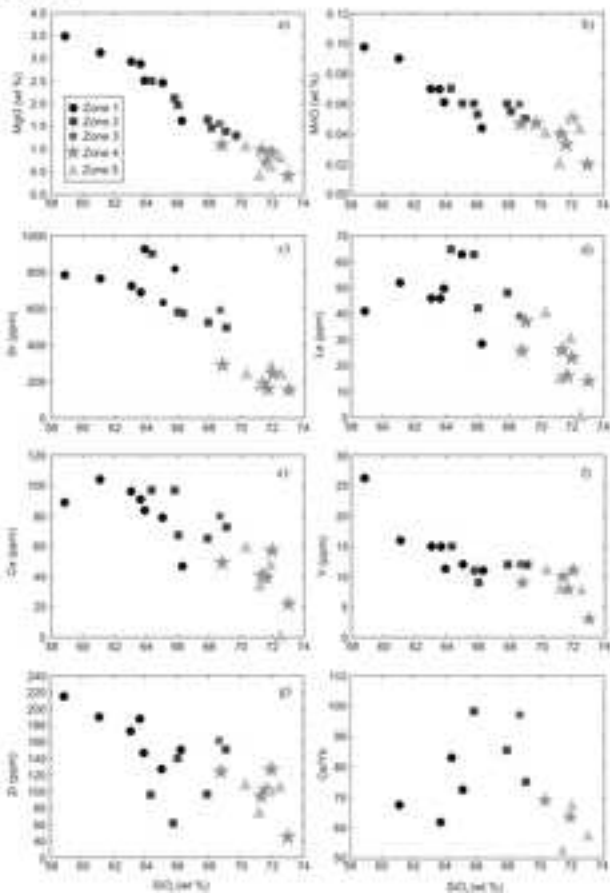


Figure 5

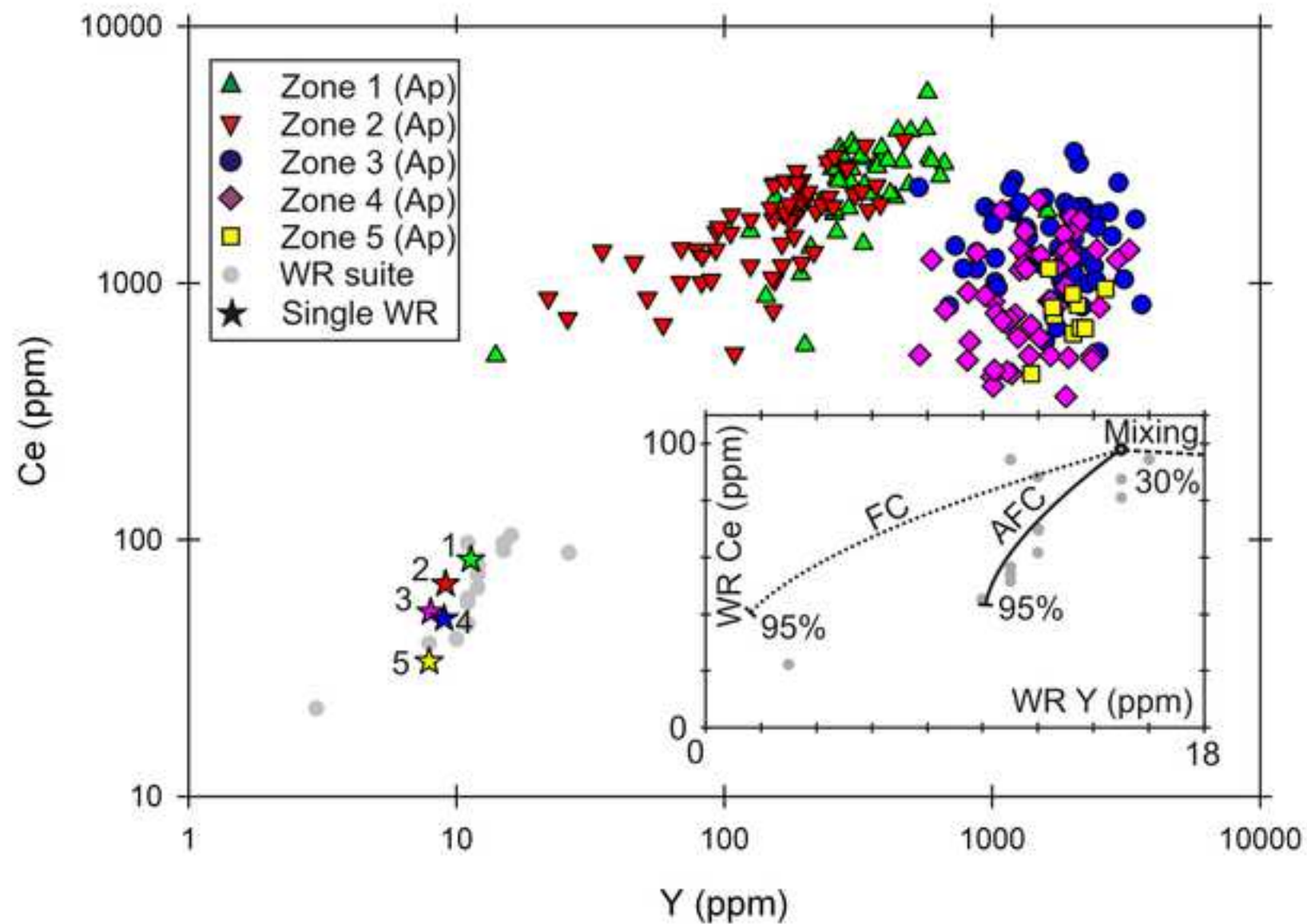


Figure 6

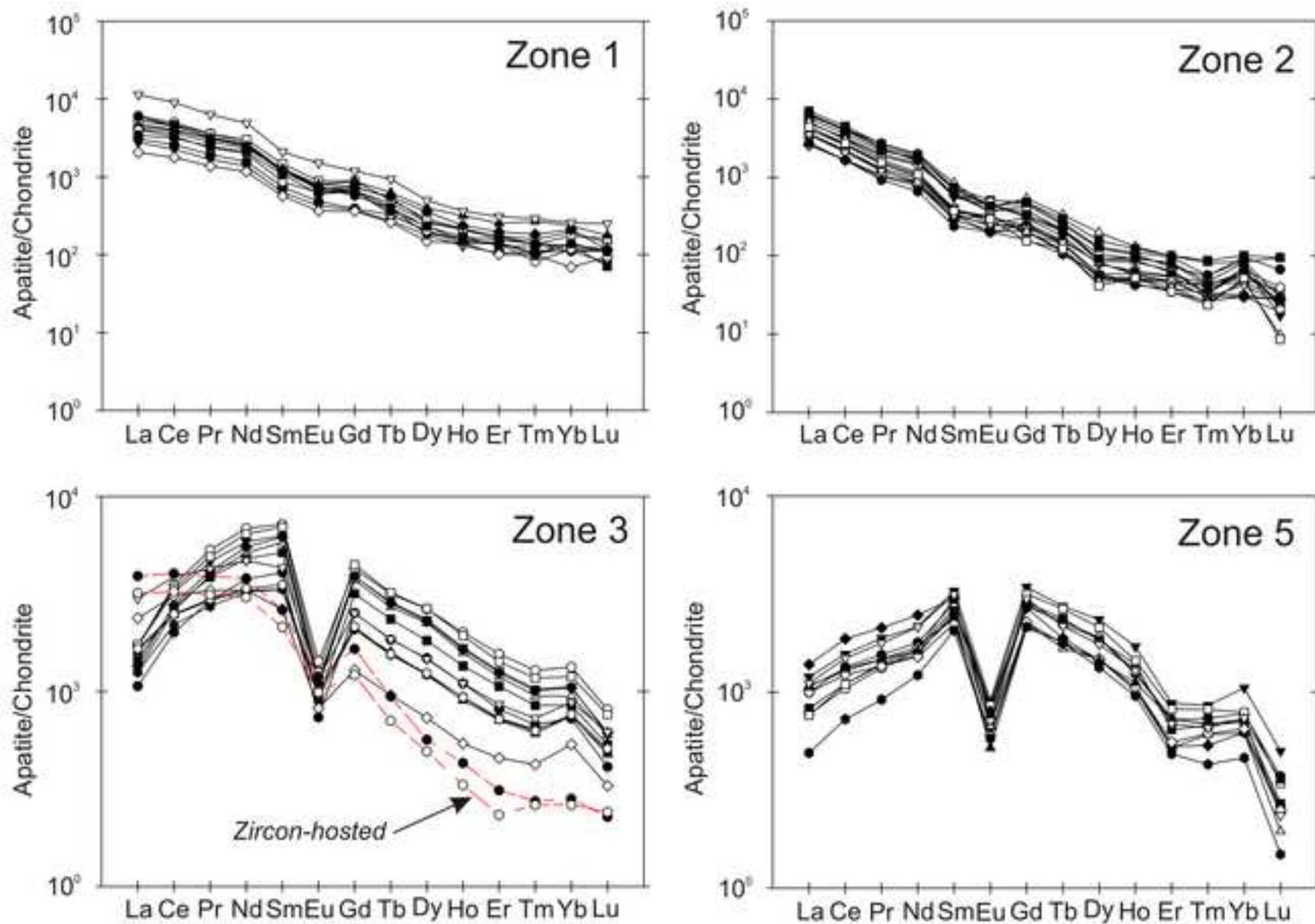


Figure 7

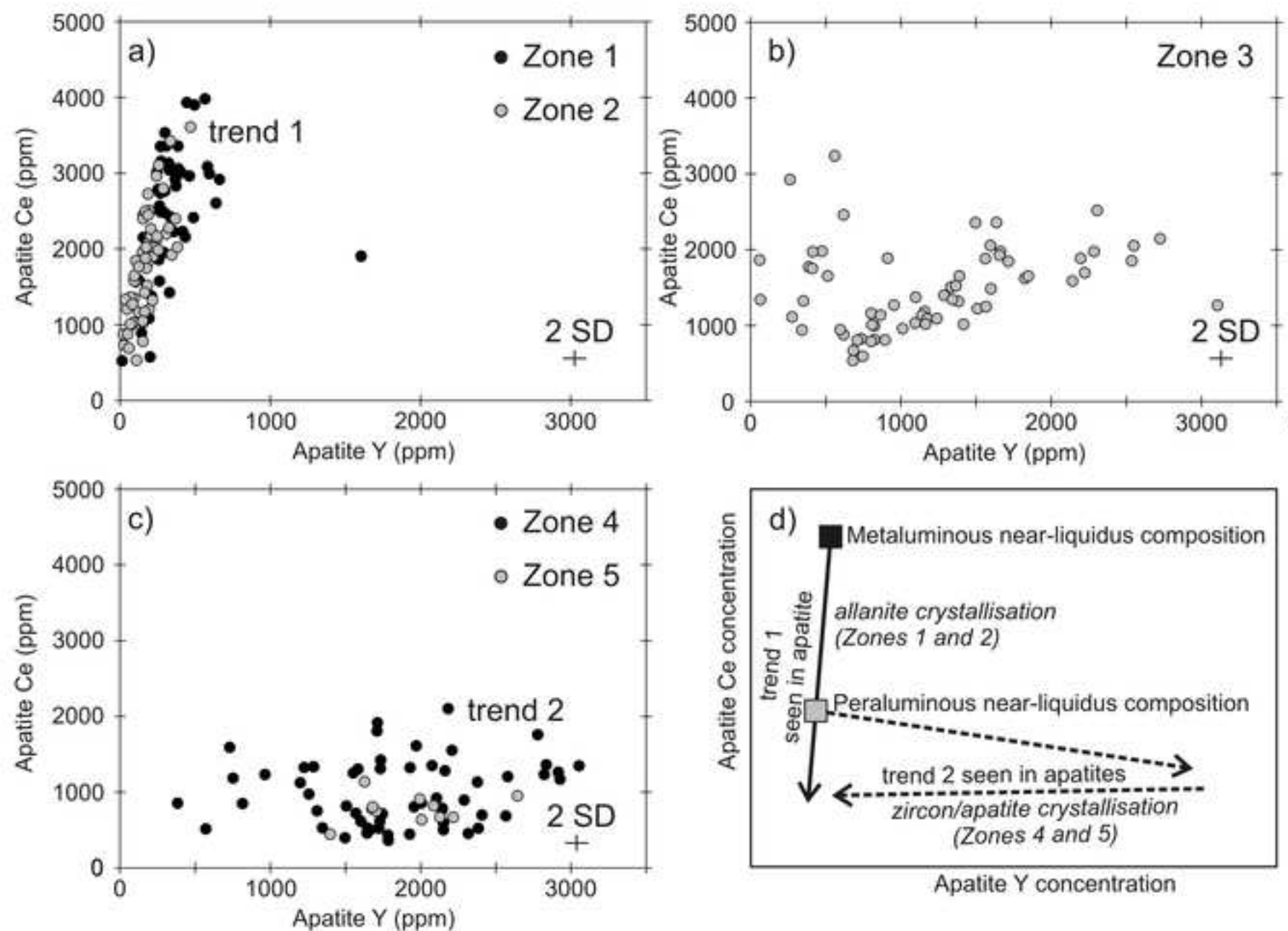


Figure 8

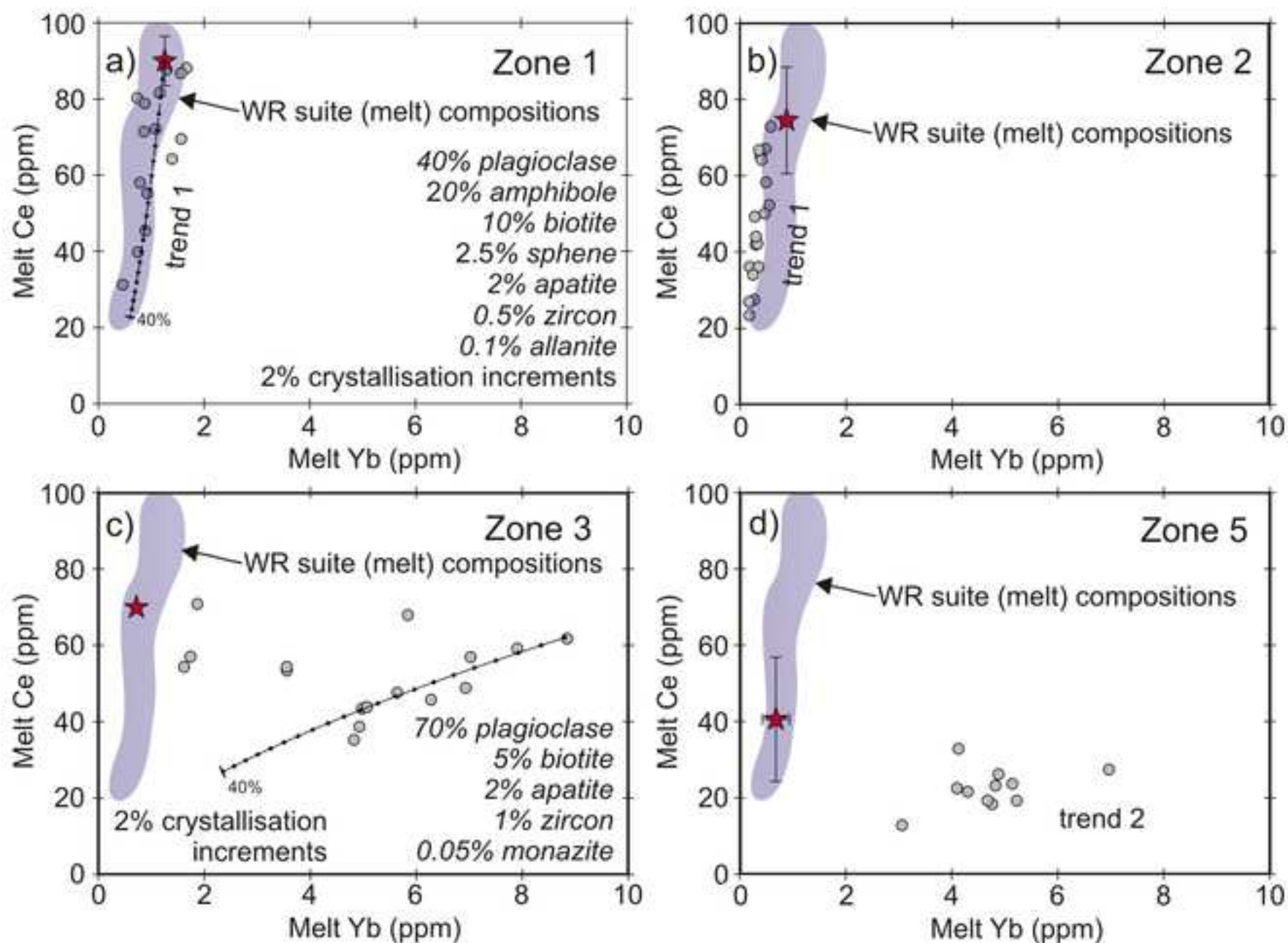


Figure 9

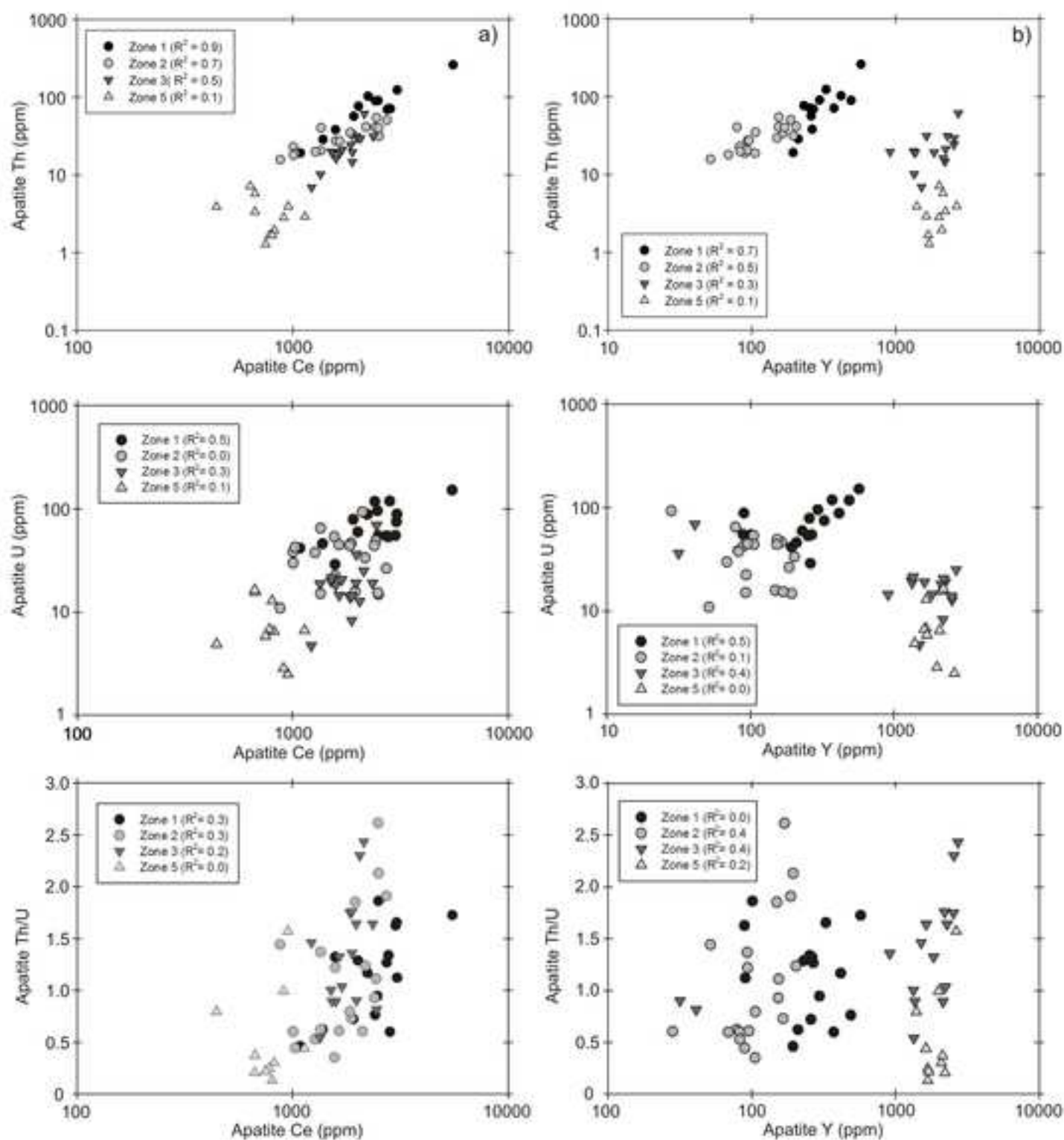


Figure 10

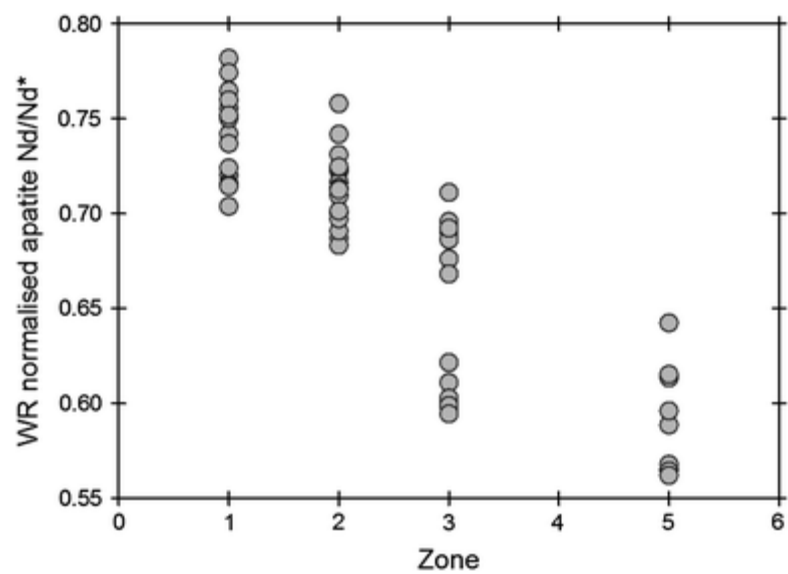


Figure 11

